Nodal Discrete Duality numerical scheme for nonlinear diffusion problems on general meshes

Boris Andreianov, El Houssaine Quenjel

Nodal Discrete Duality numerical scheme for nonlinear diffusion problems on general meshes

Boris Andreianov[1] and El Houssaine Quenjel [2]

[1]Institut Denis Poisson CNRS UMR7013, Université de Tours, Université d'Orléans, Parc Grandmont, 37200 Tours, France and Peoples' Friendship University of Russia (RUDN University), 6 Miklukho-Maklaya St, Moscow, 117198, Russian Federation, boris.andreianov@univ-tours.fr

[2]Chair of Biotechnology, LGPM, CentraleSupélec, CEBB, 3 rue des Rouges Terres, 51110 Pomacle, France, el-houssaine.quenjel@centralesupelec.fr

July 28, 2022

Abstract

DDFV (Discrete Duality Finite Volume) schemes are known for their ability to approximate nonlinear and linear anisotropic diffusion operators on general meshes, but they possess several drawbacks. The most important drawback of DDFV is the simultaneous use of the cell and the node unknowns. We propose a discretization approach that incorporates DDFV ideas and the associated analysis techniques, but allows for a rapid elimination of the cell unknowns. Further, unlike the DDFV scheme, the new "Nodal Discrete Duality" (NDD) scheme does not require specific adaptation in presence of discontinuities of the diffusion tensor along cell boundaries.

We describe in detail the 2D NDD framework and its two 3D variants, focusing on the consistency properties of the discrete gradient and discrete divergence operators and on the key structural property of Discrete Duality. For the 2D scheme, convergence analysis is carried out and a series of numerical tests are provided for a large family of nonlinear anisotropic elliptic problems with zero Dirichlet boundary condition.

Key words : Nodal scheme, diamond scheme, discrete duality, general meshes, nonlinear elliptic equation, p-Laplacian, coercivity, consistency, convergence, 3D scheme.

AMS subject classifications : 35K55, 35K65, 65M08, 65M12.

1 Introduction

Since more than twenty years, approximation of diffusion operators in the context of anisotropy and/or nonlinearity and/or general meshes was an important subject of research in numerical analysis for PDEs, in particular in the context of Finite Volume methods. We refer to the survey [20], to the benchmarks [26, 25] and references therein for extensive information on a number of methods designed to handle such diffusion problems on general meshes. Among the numerical methods designed for this purpose, many popular approaches enter the framework of gradient schemes; we refer to the book [21] for a detailed exposition of the theory and practice of gradient schemes.

1.1 DDFV schemes and the specificity of the new NDD scheme

One of the key features of the gradient schemes is their asymptotic consistency with the Stokes (Green-Gauss) integration-by-parts formula. Some numerical schemes are exactly consistent with the Stokes (Green-Gauss) formula. This includes mimetic schemes [14, 32], the Control Volume Finite Element (co-volume)

scheme of [15, 1] (see in particular [4, 9] for the Discrete Duality feature). A particular instance of exactly consistent with integration-by-parts schemes took the name of Discrete Duality Finite Volume (DDFV) schemes. In 2D, they were discovered in [27, 28] then rediscovered and firmly established in [18], see also [8]. Three-dimensional DDFV schemes were proposed in [29, 17, 3] (for the version called 3D CeVe-DDFV) and in [16] (for the version called 3D CeVeFE-DDFV). In the context of parabolic reaction-diffusion problems, DDFV schemes are not exactly gradient schemes due to the peculiarities of the definition of discrete functions and of their scalar product. For the simplest elliptic linear problems, they do reduce to gradient schemes, see [22, Sect. 3.5]; note that the modification proposed in [2, Appendix B] (cf. the discussion in [22, Sect. 2.1]) makes DDFV a gradient scheme in a more general context including reaction terms. In general, even if in all situations the DDFV schemes remain quite close to the gradient schemes' paradigm, they possess an analysis machinery of their own. The latter relies in essential way on the appropriate consistency properties of discrete operators and upon the Discrete Duality property.

DDFV schemes proved performant, especially in what concerns the quality of the gradient approximation, in the benchmarks [26, 25]. They possess however several drawbacks, in particular the following:

- DDFV schemes are based upon the simultaneous use of degrees of freedom (DOFs, in the sequel) located both at the nodes and at the centers of the mesh (called *primal* mesh in the DDFV formalism). Compared to most other methods that use either the node DOFs or the center DOFs, this leads to a larger algebraic system to solve, while the benefit of a finer resolution for approximating the solution in L^p norms is not clear[1]. We particularly stress the fact that the resulting system is strongly coupled, not allowing for elimination of either of the two families of DOFs.
- The case of spatially heterogeneous, piecewise continuous diffusion tensor was successfully addressed in [11] under the name of m-DDFV. The resulting method is precise but it is somewhat complex and cumbersome, requiring resolution of auxiliary 2×2 systems for every interface where the diffusion tensor has a jump. This is particularly true for nonlinear problems like (1.1), where the resulting local systems are nonlinear.
- The convergence analysis of DDFV schemes, beyond the simplest case of pure diffusion problems like in [8], is jeopardized by the difficulty to prove that the two components of the solution, usually called $u^{\mathcal{M}}$ and $u^{\mathcal{M}^\star}$, converge to the same limit. The introduction of a penalization operator [5] introduces an additional mild coupling between the center and the node DOFs that solves this theoretical difficulty. However penalization terms make heavier both the implementation and the presentation of the scheme, while all the numerical tests the authors are aware of illustrate the fact that the penalization is not useful in practice.

The aim of this work is to develop and study a new numerical scheme which construction is inspired by the DDFV methodology. We claim that this new scheme is numerically efficient (boiling down, in practice, to a nodal scheme) and easy to analyze within the DDFV formalism. Indeed, we preserve the mimetic feature of the scheme (the Discrete Duality property), thus greatly facilitating the convergence analysis; and we preserve the DDFV approach to the gradient discretization on a "diamond mesh", leading to a high-quality approximation of the solution gradient. The construction of this new scheme involves both the node and the center DOFs; but the center ones, being connected only to the surrounding node DOFs, can be locally eliminated at a low numerical cost - for nonlinear problems, this is done at the level of each Newton iteration. Thus in practice, our approach has the complexity of a pure nodal scheme. For these reasons, we call it NDD (for *Nodal Discrete Duality*) scheme. Further, the NDD scheme takes into account the jump discontinuities of the diffusion tensor without any specific adaptation, due to the fact that (as compared to m-DDFV) the diamonds do not include the edges of the primal mesh along which the diffusion tensor discontinuities can occur. This simplification is analogous to the one highlighted in [22, Rem. 3.7]. Furthermore, the analysis of the NDD scheme does not require the introduction of a penalization operator, unlike for DDFV schemes. Finally, as for the case of 2D DDFV schemes, the idea of 2D NDD scheme extends to 3D: we propose two variants of such extension, inspired by the two known 3D DDFV schemes.

[1] the DDFV approximation of the fluxes does present a benefit; in particular, the DDFV method guarantees strongly convergent fluxes for linear and non-linear diffusion problems ([8]), contrary to some simpler and classical schemes, and a good accuracy of gradient and fluxes is witnessed through numerical tests ([26, 25])

The price we pay for these properties, advantageous in the light of the above shortcomings of the DDFV schemes, is that we abandon the Finite Volume nature of the scheme. This means that, although the discrete equations are obtained from integration of the divergence term on each mesh cell and on each dual mesh cell (before elimination of the unknowns corresponding to the mesh centers) via the use of the Stokes (Green-Gauss) theorem, the fluxes across cell boundaries are *non-conservative*; this is due to the fact that the reconstructed flux jumps across the interfaces of the mesh. Let us stress however that the Discrete Duality feature, which is an avatar of the integration-by-parts procedure, holds true for the NDD discrete operators of gradient and divergence; this feature underlies the convergence analysis of the NDD method, which is mimicked from the DDFV convergence analysis. While in the standard DDFV paradigm the Discrete Duality was a convenient global expression of the flux conservativity property, in our NDD scheme we loose the flux conservativity without giving up the key feature of Discrete Duality.

1.2 The PDE context used to illustrate the NDD discretization approach

For the sake of illustrating the NDD construction and the convergence analysis, in this paper we consider solving the second-order nonlinear elliptic problem

$$\begin{cases} -\operatorname{div} \boldsymbol{\alpha}(x, \nabla u) = f & \text{in } \Omega \\ u = 0 & \text{on } \partial\Omega \end{cases}, \tag{1.1}$$

on a bounded connected polygonal domain $\Omega \subset \mathbb{R}^2$ with a Lipschitz continuous boundary $\partial\Omega$.

We set up the assumptions on the problem data. They are required to identify the functional spaces allowing to give a proper sense to the solution. Let $p \in (1, +\infty)$, the conjugate of p will be denoted by $p' = p/(p-1)$.

$(\mathbf{H}_1)$ The nonlinearity $\boldsymbol{\alpha} : \Omega \times \mathbb{R}^2 \to \mathbb{R}^2$ is of Caratheodory kind and satisfies the following properties.

- There exist $C_{\boldsymbol{\alpha}}, C'_{\boldsymbol{\alpha}} > 0$ and $m_0 \in L^1(\Omega), m'_0 \in L^{p'}(\Omega)$ such that

$$\boldsymbol{\alpha}(\cdot, \zeta) \cdot \zeta \geq C_{\boldsymbol{\alpha}} |\zeta|^p - m_0, \quad \forall \zeta \in \mathbb{R}^2, \tag{1.2a}$$

$$|\boldsymbol{\alpha}(\cdot, \zeta)| \leq C'_{\boldsymbol{\alpha}} |\zeta|^{p-1} + m'_0, \quad \forall \zeta \in \mathbb{R}^2. \tag{1.2b}$$

- $\boldsymbol{\alpha}$ is strictly monotone with respect to the second variable i.e.

$$\Big(\boldsymbol{\alpha}(\cdot, \zeta) - \boldsymbol{\alpha}(\cdot, \zeta')\Big) \cdot \big(\zeta - \zeta'\big) > 0, \quad \forall \zeta \neq \zeta' \in \mathbb{R}^2. \tag{1.2c}$$

$(\mathbf{H}_2)$ The right hand side f is in $L^{p'}(\Omega)$.

Based on these assumptions, it can be checked that $\boldsymbol{\alpha}$ gives rise to a Nemytskii operator from $L^p(\Omega)^2$ into $L^{p'}(\Omega)^2$. Maps satisfying **$(\mathbf{H}_1)$**-**$(\mathbf{H}_2)$** are often called Leray-Lions operators in the literature. An example of such an operator is the anisotropic p-Laplacian governed by

$$\boldsymbol{\alpha}(\cdot, \zeta) = \begin{cases} \Big(\Lambda(\cdot)\zeta \cdot \zeta\Big)^{\frac{p-2}{2}} \Lambda(\cdot)\zeta & \forall \zeta \in \mathbb{R}^2 \setminus 0 \\ 0 & \text{for } \zeta = 0 \end{cases}, \tag{1.3}$$

where $x \in \Omega \to \Lambda(x) \in L^\infty(\Omega)^{2\times 2}$ is positive-definite matrix, which is uniformly coercive. In the case where Λ is the identity matrix, we recover the standard p-Laplacian operator.

The solution to the continuous problem is understood in the weak sense.

Definition 1.1. *A weak solution to the mathematical model* (1.1) *is any function* $u \in W_0^{1,p}(\Omega)$ *satisfying the variational formulation*

$$\int_\Omega \boldsymbol{\alpha}(x, \nabla u) \cdot \nabla \psi \, \mathrm{d}x = \int_\Omega f\psi \, \mathrm{d}x, \quad \forall \psi \in \mathcal{C}_c^\infty(\Omega). \tag{1.4}$$

We recall that the equation (1.1) is uniquely solvable in $W_0^{1,p}(\Omega)$. The proof can be documented in [30].

Theorem 1.1. *Under Assumptions* ***$(\boldsymbol{H}_1)$***-***$(\boldsymbol{H}_2)$****, there exists a unique solution to* (1.1) *in the sense of Definition 1.1.*

1.3 Outline of the paper

The paper is organized as follows. In Section 2, we describe the 2D NDD framework with meshing, the associated spaces of discrete functions and discrete vector-fields, the discrete operators of gradient and divergence. We pay a particular attention to the Discrete Duality relation for these operators and to their consistency properties. In Section 3, we make precise the NDD discretization for problem (1.1), establish *a priori* estimates and the well-posedness of the scheme, and describe the elimination of the cell unknowns. In Section 4 we outline the convergence analysis for the NDD discretization of (1.1). In Section 5 we describe two 3D versions of the NDD construction, focusing again on the key duality and consistency properties. Section 6 is devoted to numerical tests for the 2D NDD scheme. Finally, Section 7 concludes the paper.

2 The discrete functional context for the NDD scheme

The construction and the analysis of the NDD scheme requires the definition of several geometrical objects, the associated discrete spaces and the operators like in the DDFV setting ([27, 28, 18, 8], we construct primal, dual and diamond meshes; DOFs will be associated to primal and dual volumes and give rise to discrete functions, while the diamonds will serve to define discrete fields such as gradients of discrete functions and the fluxes of the discretized PDE (1.1). In what follows, we define the meshes and the discrete functions; the discrete gradient operator acting from the space of discrete functions to the one of discrete vector-fields; and the discrete divergence operator acting in the converse way.

2.1 Meshing, DOFs and discrete functions.

The NDD construction starts from a primal mesh $\mathfrak{M}$, which is a collection of convex polygons partitioning (up to a subset of measure zero) the domain Ω. The elements of $\mathfrak{M}$ are referred to as cells or as control volumes. For every cell $A \in \mathfrak{M}$, we denote by $|A|$ its measure, by x_A its mass center and by h_A its diameter. The set of edges of A is designated by $\mathcal{E}_A$, σ stands for a generic edge. In the case where σ separates cells A and B, i.e., $\mathcal{E}_A \cap \mathcal{E}_B = \{\sigma\}$, we also use the notation $A|B$ for the edge σ. Let $\sigma \in \mathcal{E}_A$. We denote by $|\sigma|$ length of σ, x_σ its center, by $\mathbf{n}_{A,\sigma}$ the unit normal to σ pointing outward A, and by $\mathbf{N}_{A,\sigma}$ we denote the normal vector weighted by the length of the interface:

$$\mathbf{N}_{A,\sigma} := |\sigma| \mathbf{n}_{A,\sigma}.$$

Finally, we denote by ν_σ the the set of all vertices of σ.

The dual mesh $\overline{\mathfrak{M}^\star}$ is derived from the primal one and it is constructed around its vertices (see Figure 1, see [8] for details). For each vertex $x_{A^\star}$ we associate a unique dual control volume $A^\star$ built by connecting the cell centers to the mid point of the interfaces sharing the same vertex $x_{A^\star}$. We denote by $|A^\star|$ its volume and by $h_{A^\star}$ its diameter. The set $\mathcal{E}_{A^\star}$ stands for the interfaces of $A^\star$. The length of $\sigma^\star \in \mathcal{E}_{A^\star}$ is denoted by $|\sigma^\star|$. For $A \in \mathfrak{M}$, $\sigma \in \mathcal{E}_A$ there exists a unique dual interface $\sigma^\star$ included into the convex envelope $\mathcal{D}_{A,\sigma}$ of x_A and σ (see the below description of diamonds); we denote this dual interface $\sigma^\star_{A,\sigma}$ (see Fig. 2). The unit vector normal to $\sigma^\star_{A,\sigma}$ and pointing outside $A^\star$ is denoted by $\mathbf{n}^{A^\star}_{A,\sigma}$, and the corresponding normal vector weighted by the length of the dual interface $\sigma^\star_{A,\sigma}$ is

$$\mathbf{N}^{A^\star}_{A,\sigma} := \left|\sigma^\star_{A,\sigma}\right| \mathbf{n}^{A^\star}_{A,\sigma}.$$

As in DDFV methods, discrete fields will be expressed on a third mesh, called the diamond mesh[2]. The diamonds of the NDD scheme are pictured in Figure 2; they are labeled by couples $(A, \sigma) \in \mathfrak{M} \times \mathcal{E}$ such that $\sigma \in \mathcal{E}_A$. For each $A \in \mathfrak{M}$, for each $\sigma \in \mathcal{E}_A$, we define $\mathcal{D}_{A,\sigma}$ to be the cone with vertex x_A and basis σ; in other words, $\mathcal{D}_{A,\sigma}$ is the triangle whose vertices are x_A and the extremities of σ. In a generic diamond, we will write $x_{A^\star_\sigma}$ and $x_{B^\star_\sigma}$ for the vertices of σ, and $x_\sigma = \frac{1}{2}(x_{A^\star_\sigma} + x_{B^\star_\sigma})$ for the center of σ. Further, for each diamond $\mathcal{D} = \mathcal{D}_{A,\sigma}$ associated with a primal edge σ, we define the dual edge $\sigma^\star_{A,\sigma} := [x_A, x_\sigma]$ (this is the median of the triangle $\mathcal{D}_{A,\sigma}$ starting at x_A). For a given interface σ, the orientation (i.e., the choice of the one of the two vertices that will be labeled $x_{A^\star_\sigma}$) is fixed in an arbitrary way. Then, $\mathbf{n}^\star_{A,\sigma}$ will denote

[2]Note that the diamond mesh of our NDD method corresponds to the half-diamonds of the standard DDFV scheme [18, 8].

the unit normal vector to $\sigma^\star_{A,\sigma}$ making an angle $\theta_{A,\sigma} \in]0, \pi/2]$ with the vector pointing from $x_{A^\star_\sigma}$ to $x_{B^\star_\sigma}$; and $\mathbf{N}^\star_{A,\sigma} = \left|\sigma^\star_{A,\sigma}\right| \mathbf{n}^\star_{A,\sigma}$ is the corresponding weighted normal. Note that the measure of $\mathcal{D}_{A,\sigma}$ is given by

$$|\mathcal{D}_{A,\sigma}| = \frac{1}{2} \left|\sigma^\star_{A,\sigma}\right| |\sigma| \sin(\theta_{A,\sigma}).$$

For a generic diamond $\mathcal{D}$, we denote by $h_\mathcal{D}$ the diameter of $\mathcal{D}$.

Remark 2.1. *We highlight the fact that two different notations will be used for dual normals. On the one hand, in the context of the discrete gradient operator and in summations performed per diamond, the quantities $\mathbf{N}^\star_{A,\sigma}$ appear in a natural way. On the other hand, in the context of the discrete divergence operator and of summations performed per dual volume, the notation $\mathbf{N}^{A^\star}_{A,\sigma}$ is necessary. To handle this notation redundancy properly, observe that*

$$\mathbf{N}^{A^\star}_{A,\sigma} = +\mathbf{N}^\star_{A,\sigma} \text{ if } A^\star = A^\star_\sigma, \quad \text{and} \quad \mathbf{N}^{A^\star}_{A,\sigma} = -\mathbf{N}^\star_{A,\sigma} \text{ if } A^\star = B^\star_\sigma. \tag{2.1}$$

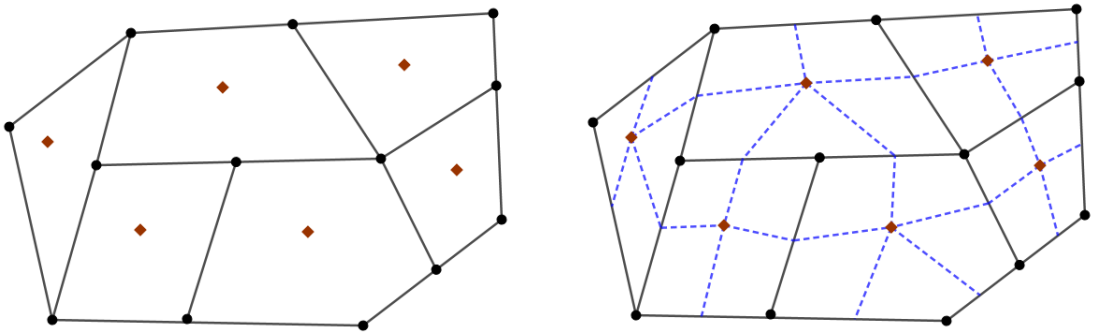

Figure 1: The primal mesh $\mathfrak{M}$ (solid lines); and the dual mesh $\overline{\mathfrak{M}^\star}$ (dashed lines).

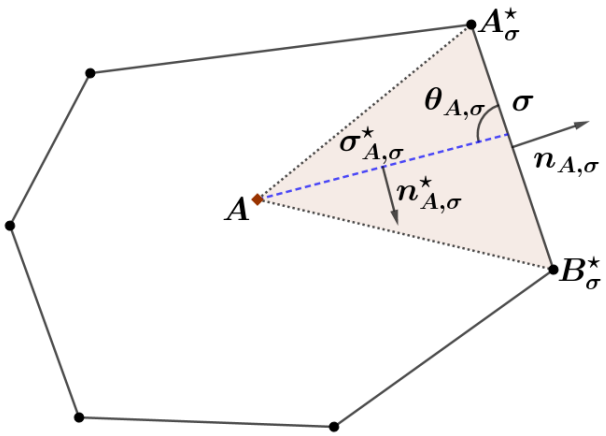

Figure 2: A generic diamond $\mathcal{D}_{A,\sigma}$ with the associated notations.

We further need to suppose a regularity requirement on the mesh to control in particular the flatting of the diamond cells. The mesh regularity is defined, per diamond $\mathcal{D} = \mathcal{D}_{A,\sigma}$, by

$$\theta^{\mathcal{D}_{A,\sigma}} = \max\left\{\frac{1}{\sin(\theta_{A,\sigma})}, \frac{h_{\mathcal{D}_{A,\sigma}}}{\sqrt{|\mathcal{D}_{A,\sigma}|}}, \max_{K \in \{A, A^\star_\sigma, B^\star_\sigma\}} \frac{h_K}{\sqrt{|K|}}\right\}.$$

In the rest of this paper we assume that there exists a constant $\overline{\theta}$ such that

$$\theta^\mathcal{D} \leq \overline{\theta}, \quad \forall \mathcal{D} \in \mathfrak{D}. \tag{2.2}$$

As usual in the DDFV formalism, within $\overline{\mathfrak{M}^\star}$, we distinguish the set $\mathfrak{M}^\star$ of interior dual cells and write $\partial\mathfrak{M}^\star = \overline{\mathfrak{M}^\star} \setminus \mathfrak{M}^\star$ for the set of the dual cells that have an edge included in $\partial\Omega$. Note that contrary to the DDFV framework, in the NDD method we do not need to introduce the family $\partial\mathfrak{M}$ of degenerate boundary volumes. A generic primal or dual interior cell of the mesh (i.e., a generic element of $\mathcal{T} = \mathfrak{M} \cup \mathfrak{M}^\star$) will be denoted by K. DOFs will be associated to $K \in \mathfrak{M} \cup \mathfrak{M}^\star$ (prior to the algebraic elimination of the unknowns corresponding to $K = A \in \mathfrak{M}$) and one balance equation per primal or dual interior cell K will be written. At the same time, the DOFs that would correspond to the volumes in $\partial\mathfrak{M}^\star$ will be fixed to zero, thus accounting for the Dirichlet boundary condition in (1.1). Note that other boundary conditions can be taken into consideration, within the same DDFV formalism. Finally the size of an NDD mesh is taken to be

$$h^{\mathcal{T}} = \max\left(\max_{A\in\mathfrak{M}} h_A,\ \max_{A^\star\in\overline{\mathfrak{M}^\star}} h_{A^\star},\ \max_{\mathcal{D}\in\mathfrak{D}} h_{\mathcal{D}}\right).$$

Introduce $\mathbb{R}^{\mathcal{T}}$, $\mathbb{R}^{\overline{\mathcal{T}}}$ the spaces where the primal and dual unknowns (the DOFs of the method) and the boundary values live. The sets $\mathbb{R}^{\mathcal{T}}$, $\mathbb{R}^{\overline{\mathcal{T}}}$ contain, respectively, elements of the form

$$v^{\mathcal{T}} = \left((v_A)_{A\in\mathfrak{M}}, (v_{A^\star})_{A^\star\in\mathfrak{M}^\star}\right) \in \mathbb{R}^{\mathcal{T}} \quad \text{and} \quad v^{\overline{\mathcal{T}}} = \left((v_A)_{A\in\mathfrak{M}}, (v_{A^\star})_{A^\star\in\overline{\mathfrak{M}^\star}}\right) \in \mathbb{R}^{\overline{\mathcal{T}}}.$$

The space $\mathbb{R}^{\mathcal{T}}$ can be identified with the subspace $\mathbb{R}_0^{\overline{\mathcal{T}}}$ of $\mathbb{R}^{\overline{\mathcal{T}}}$ such that $v^\star_A = 0$ for all $A^\star \in \partial\mathfrak{M}^\star$. Due to this identification, the notation $v^{\overline{\mathcal{T}}}$ will stand for the extension of $v^{\mathcal{T}} \in \mathbb{R}^{\mathcal{T}}$ by zero values in the boundary volumes. The space $\mathbb{R}^{\mathcal{T}}$ is endowed with the scalar product

$$\left[\!\left[v^{\mathcal{T}}, w^{\mathcal{T}}\right]\!\right]_{\mathcal{T}} = \frac{1}{2}\sum_{A\in\mathfrak{M}} |A|\, v_A w_A + \frac{1}{2}\sum_{A^\star\in\mathfrak{M}^\star} |A^\star|\, v_{A^\star} w_{A^\star}.$$

Performing the convergence analysis of the scheme requires to introduce reconstruction functions which are piecewise constant on the primal and dual meshes. Given a vector $v^{\mathcal{T}} \in \mathbb{R}^{\mathcal{T}}$ we define

$$v^{\mathfrak{M}}(x) = v_A \ \forall x \in A,\ \forall A \in \mathfrak{M}\,; \quad v^{\overline{\mathfrak{M}^\star}}(x) = v_{A^\star} \ \forall x \in A^\star,\ \forall A^\star \in \overline{\mathfrak{M}^\star},\ \text{with } v_{A^\star} = 0 \text{ if } A^\star \in \partial\mathfrak{M}^\star, \quad (2.3)$$

which are identified to two elements of $L^2(\Omega)$ (note that each of the meshes $\mathfrak{M}$, $\overline{\mathfrak{M}^\star}$ forms a partition of Ω up to a set of measure zero). Whenever useful, we will still identify $v^{\mathcal{T}}$ with the $L^2(\Omega)$-function $x \mapsto v^{\mathcal{T}}(x)$ that combines both $v^{\mathfrak{M}}$ and $v^{\overline{\mathfrak{M}^\star}}$ in the following way:

$$v^{\mathcal{T}}(x) = \frac{1}{2}\big((v^{\mathfrak{M}}(x) + v^{\overline{\mathfrak{M}^\star}}(x)\big). \quad (2.4)$$

Note that this precise reconstruction naturally appears in the compactness analysis for DDFV schemes.

2.2 Discrete vector-fields and the NDD discrete gradient operator.

In addition to the space $\mathbb{R}^{\mathcal{T}}$ of discrete functions, we introduce $(\mathbb{R}^2)^{\mathfrak{D}}$ the space of discrete vector-fields on Ω. Each element $\mathcal{F}^{\mathfrak{D}}$ of $(\mathbb{R}^2)^{\mathfrak{D}}$ writes $\mathcal{F}^{\mathfrak{D}} = (\mathcal{F}_{\mathcal{D}})_{\mathcal{D}\in\mathfrak{D}}$, i.e., discrete vector-fields are constant per diamond. This space is equipped with the scalar product

$$\left\{\!\!\left\{\mathcal{F}^{\mathfrak{D}}, \mathcal{G}^{\mathfrak{D}}\right\}\!\!\right\}_{\mathfrak{D}} = \sum_{\mathcal{D}\in\mathfrak{D}} |\mathcal{D}|\, \mathcal{F}_{\mathcal{D}} \cdot \mathcal{G}_{\mathcal{D}}.$$

Now the NDD discrete gradient operator $\nabla^{\mathfrak{D}} : \mathbb{R}_0^{\overline{\mathcal{T}}} \to (\mathbb{R}^2)^{\mathfrak{D}}$ is defined as follows. First, let us set

$$v_\sigma = \frac{1}{2}\big(v_{A^\star_\sigma} + v_{B^\star_\sigma}\big), \quad \forall \sigma \in \mathcal{E}. \quad (2.5)$$

Then for every $v^{\mathcal{T}} \in \mathbb{R}^{\mathcal{T}}$ we define in each diamond $\mathcal{D} = \mathcal{D}_{A,\sigma}$

$$\nabla_{\mathcal{D}_{A,\sigma}} v^{\overline{\mathcal{T}}} = \frac{1}{\sin(\theta_{A,\sigma})}\left(\frac{v_\sigma - v_A}{|\sigma^\star_{A,\sigma}|}\mathbf{n}_{A,\sigma} + \frac{v_{B^\star_\sigma} - v_{A^\star_\sigma}}{|\sigma|}\mathbf{n}^\star_{A,\sigma}\right), \quad \forall A \in \mathfrak{M}\ \forall \sigma \in \mathcal{E}_A. \quad (2.6)$$

We can therefore associate to a discrete function $v^{\mathcal{T}}$ its discrete gradient denoted by $\nabla^{\mathfrak{D}} v^{\overline{\mathcal{T}}}$; whenever this is convenient, the discrete vector-field $\nabla^{\mathfrak{D}} v^{\overline{\mathcal{T}}}$ will be identified to an $\mathbb{R}^2$-valued function on Ω as follows:

$$\nabla^{\mathfrak{D}} v^{\overline{\mathcal{T}}}(x) = \nabla_{\mathcal{D}}\, v^{\overline{\mathcal{T}}} \quad \forall x \in \mathcal{D},\ \forall \mathcal{D} \in \mathfrak{D}.$$

In practice we take advantage of the following equivalent formula of the discrete gradient instead of the previous one (2.6):

$$\nabla_{\mathcal{D}_{A,\sigma}} v^{\overline{\mathcal{T}}} = \frac{1}{2\,|\mathcal{D}_{A,\sigma}|}\Big((v_\sigma - v_A)\,\mathbf{N}_{A,\sigma} + (v_{B^\star_\sigma} - v_{A^\star_\sigma})\mathbf{N}^\star_{A,\sigma}\Big), \quad \text{for } \mathcal{D} = \mathcal{D}_{A,\sigma} \in \mathfrak{D}, \tag{2.7}$$

where we recall the notation (see also Remark 2.1)

$$\mathbf{N}_{A,\sigma} = |\sigma|\,\mathbf{n}_{A,\sigma}, \qquad \mathbf{N}^\star_{A,\sigma} = \big|\sigma^\star_{A,\sigma}\big|\,\mathbf{n}^\star_{A,\sigma}.$$

Remark 2.2. *We highlight the fact that due to the definition of v_σ in* (2.5)*, formulas* (2.6),(2.7) *boil down to the $\mathbb{P}_1$ finite elements gradient on the triangle whose vertices are $A, A^\star_\sigma, B^\star_\sigma$. This ensures, in particular, the exactness of the discrete gradient on affine functions. However, in our analysis, conducted within the DDFV formalism, we will not further exploit this appealing feature of the NDD scheme.*

Proposition 2.1. *Denote by $\mathbb{P}^{\overline{\mathcal{T}}}$ the operator of projection of a smooth function on $\mathbb{R}^{\overline{\mathcal{T}}}$: for $\varphi \in C^\infty_0(\Omega)$, $\mathbb{P}^{\overline{\mathcal{T}}}\varphi$ has the entries $\varphi(x_K)$ at cells $K \in \mathfrak{M} \cup \mathfrak{M}^\star$, and zero values at boundary cells. The NDD discrete gradient operator $\nabla^{\mathfrak{D}}$ is consistent in the sense that $\|\nabla^{\mathfrak{D}}\mathbb{P}^{\overline{\mathcal{T}}}\varphi - \nabla\varphi\|_\infty \to 0$ as the size $h^{\mathcal{T}}$ of $\mathcal{T}$ goes to zero, under the assumption* (2.2) *with some mesh-independent bound $\overline{\theta}$ of the regularity indicator.*

The proof is straightforward, combining the exactness of the discrete gradient (2.6),(2.7) on functions that are affine per diamond (this is obvious from Remark 2.2) and standard approximation of $\varphi|_{\mathcal{D}_{A,\sigma}}$ by its first-order Taylor expansion at x_σ (see, e.g., [2, Prop. 3.5(ii)]).

2.3 The NDD discrete divergence operator and Discrete Duality.

The NDD discrete divergence operator $\mathrm{div}^{\mathcal{T}} : (\mathbb{R}^2)^{\mathfrak{D}} \to \mathbb{R}^{\mathcal{T}}$ is defined in a quite special way, taking into account the non-conservativity of the NDD fluxes at the primal interfaces σ. Indeed, note that the definition of NDD diamonds entails that each dual interface $\sigma^\star$ is included into a unique diamond; but each primal interface σ is the boundary between two adjacent diamonds, unless $\sigma \subset \partial\Omega$.

Consider $\mathcal{F}^{\mathfrak{D}} \in (\mathbb{R}^2)^{\mathfrak{D}}$. The discrete divergence of a discrete vector-field $\mathcal{F}^{\mathfrak{D}}$ is the collection

$$\mathrm{div}^{\mathcal{T}}\,\mathcal{F}^{\mathfrak{D}} = \Big((\mathrm{div}_A\,\mathcal{F}^{\mathfrak{D}})_{A\in\mathfrak{M}}, (\mathrm{div}_A\,\mathcal{F}^{\mathfrak{D}})_{A^\star\in\mathfrak{M}^\star}\Big).$$

The primal components of $\mathrm{div}^{\mathcal{T}}\,\mathcal{F}^{\mathfrak{D}}$ are defined by

$$\mathrm{div}_A\,\mathcal{F}^{\mathfrak{D}} := \frac{1}{|A|}\sum_{\sigma\in\mathcal{E}_A} \mathcal{F}_{\mathcal{D}_{A,\sigma}} \cdot \mathbf{N}_{A,\sigma}, \quad \forall A \in \mathfrak{M}. \tag{2.8}$$

Unlike in the DDFV context, in the dual cell the definition of the discrete divergence is not a straightforward analogue of the previous one. Our aim in introducing a non-obvious definition is to properly account for the discrete duality relationship (see Proposition 2.2); this way to define the discrete divergence can be traced back to the mimetic ideas (cf. [14]). We set

$$\mathrm{div}_{A^\star}\,\mathcal{F}^{\mathfrak{D}} := \frac{1}{|A^\star|}\sum_{A\in\mathfrak{M}_{A^\star}} \sum_{\substack{\sigma\in\mathcal{E}_A \\ A^\star\in\nu_\sigma}} \mathcal{F}_{\mathcal{D}_{A,\sigma}} \cdot \widetilde{\mathbf{N}^{A^\star}_{A,\sigma}}, \quad \forall A^\star \in \mathfrak{M}^\star, \tag{2.9}$$

where (keeping in mind Remark 2.1 on orientation of the dual normal $\mathbf{N}^{A^\star}_{A,\sigma}$) we introduce the *modified dual normal* $\widetilde{\mathbf{N}^{A^\star}_{A,\sigma}}$ by the formula

$$\widetilde{\mathbf{N}^{A^\star}_{A,\sigma}} := \mathbf{N}^{A^\star}_{A,\sigma} - \frac{1}{2}\mathbf{N}_{A,\sigma}. \tag{2.10}$$

Remark 2.3. *Let us stress that the contributions of an interface $\sigma = A|B$ to $\mathrm{div}_A \mathcal{F}^{\mathfrak{D}}$, $\mathrm{div}_B \mathcal{F}^{\mathfrak{D}}$ need not compensate, because $\mathcal{F}^{\mathfrak{D}}$ has different entries for the diamonds $\mathcal{D}_{A,\sigma}$ and $\mathcal{D}_{B,\sigma}$. In other words, the fluxes of the NDD scheme introduced below need not be conservative.*
Further, this non-conservativity impacts the definition of $\mathrm{div}_{A^\star} \mathcal{F}^{\mathfrak{D}}$. In the case of conservative fluxes, i.e., $\mathcal{F}_{\mathcal{D}_{A,\sigma}} = \mathcal{F}_{\mathcal{D}_{B,\sigma}}$ whenever $\sigma = A|B$, it is easily seen that the two contributions of $\sigma = A|B$ to $\mathrm{div}_{A^\star} \mathcal{F}^{\mathfrak{D}}$ cancel out, so that $\widetilde{\mathbf{N}_{A,\sigma}^{A^\star}}$ can be replaced by $\mathbf{N}_{A,\sigma}^{A^\star}$ in the particular case of conservative fluxes.
This observation will be crucial in proving that the above modification of the standard DDFV discrete divergence operator remains (weakly) consistent, see Proposition 2.3.

The essential feature of the NDD (Nodal Discrete Duality) scheme is the following Discrete Duality relation, that we state for the case of homogeneous Dirichlet boundary conditions.

Proposition 2.2. *The NDD discrete gradient and discrete divergence operators enjoy the following discrete duality property*

$$\forall \varphi^{\overline{\mathcal{T}}} \in \mathbb{R}_0^{\overline{\mathcal{T}}} \ \ \forall \mathcal{F}^{\mathfrak{D}} \in (\mathbb{R}^2)^{\mathfrak{D}} \qquad \Big[\!\Big[\mathrm{div}^{\mathcal{T}} \mathcal{F}^{\mathfrak{D}} \, , \, \varphi^{\mathcal{T}} \Big]\!\Big]_{\mathcal{T}} = -\Big\{\!\Big\{ \mathcal{F}^{\mathfrak{D}} \, , \, \nabla^{\mathfrak{D}} \varphi^{\overline{\mathcal{T}}} \Big\}\!\Big\}_{\mathfrak{D}}. \tag{2.11}$$

Proof. Using the definition of $\Big[\!\Big[\cdot, \cdot \Big]\!\Big]_{\mathcal{T}}$, we split the left hand side of (2.11) to obtain

$$\Big[\!\Big[\mathrm{div}^{\mathcal{T}} \mathcal{F}^{\mathfrak{D}} \, , \, \varphi^{\mathcal{T}} \Big]\!\Big]_{\mathcal{T}} = \frac{1}{2}(X + Y + Z),$$

where we separated the contribution X of $\mathfrak{M}$, and decomposed the contribution of $\mathfrak{M}^\star$ into terms Y and Z according to the right-hand side of (2.10):

$$X = \sum_{A \in \mathfrak{M}} \sum_{\sigma \in \mathcal{E}_A} \varphi_A \, \mathcal{F}_{\mathcal{D}_{A,\sigma}} \cdot \mathbf{N}_{A,\sigma}, \quad Y = \sum_{A^\star \in \mathfrak{M}^\star} \sum_{A \in \mathfrak{M}_{A^\star}} \sum_{\substack{\sigma \in \mathcal{E}_A \\ A^\star \in \nu_\sigma}} \varphi_{A^\star} \, \mathcal{F}_{\mathcal{D}_{A,\sigma}} \cdot \mathbf{N}_{A,\sigma}^{A^\star},$$

$$Z = -\frac{1}{2} \sum_{A^\star \in \mathfrak{M}^\star} \sum_{A \in \mathfrak{M}_{A^\star}} \sum_{\substack{\sigma \in \mathcal{E}_A \\ A^\star \in \nu_\sigma}} \varphi_{A^\star} \, \mathcal{F}_{\mathcal{D}_{A,\sigma}} \cdot \mathbf{N}_{A,\sigma}.$$

Bear in mind that for $A_\sigma^\star, B_\sigma^\star$ such that $\sigma = [x_{A_\sigma^\star}, x_{B_\sigma^\star}]$, in the expression Y we find the same vector $\mathcal{F}_{\mathcal{D}_{A,\sigma}}$ multiplied by the two opposite normal vectors (see (2.1)) to yield

$$\mathcal{F}_{\mathcal{D}_{A,\sigma}} \cdot \mathbf{N}_{A,\sigma}^{B_\sigma^\star} = -\mathcal{F}_{\mathcal{D}_{A,\sigma}} \cdot \mathbf{N}_{A,\sigma}^{A_\sigma^\star}, \tag{2.12}$$

which expresses the conservativity of the fluxes appearing in the sum Y. This permits to rearrange the summation of Y per diamond. Taking into account the factors $\varphi_{A_\sigma^\star}$, $\varphi_{B_\sigma^\star}$ in front of the terms (5.8), with the notation highlighted in Remark 2.1 we arrive to

$$Y = \sum_{A \in \mathfrak{M}} \sum_{\sigma \in \mathcal{E}_A} (\varphi_{A_\sigma^\star} - \varphi_{B_\sigma^\star}) \, \mathcal{F}_{\mathcal{D}_{A,\sigma}} \cdot \mathbf{N}_{A,\sigma}^\star.$$

Then, we rearrange per diamond the expression in Z before combining it with X. Observe that the same flux $\mathcal{F}_{\mathcal{D}_{A,\sigma}} \cdot \mathbf{N}_{A,\sigma}$ appears twice in the expression of Z, once with the factor $\varphi_{A_\sigma^\star}$ and another time with the factor $\varphi_{B_\sigma^\star}$. Accordingly, the expression of Z can be reordered as follows:

$$Z = -\sum_{A \in \mathfrak{M}} \sum_{\sigma \in \mathcal{E}_A} \varphi_\sigma \, \mathcal{F}_{\mathcal{D}_{A,\sigma}} \cdot \mathbf{N}_{A,\sigma}, \quad \text{where we recall that } \varphi_\sigma = \frac{1}{2}(\varphi_{A_\sigma^\star} + \varphi_{B_\sigma^\star}).$$

The summation in X is already per diamond, it naturally combines with the expression obtained for Z. Gathering the terms, we deduce

$$\frac{1}{2}(X + Y + Z) = \sum_{A \in \mathfrak{M}} \sum_{\sigma \in \mathcal{E}_A} \mathcal{F}_{\mathcal{D}_{A,\sigma}} \cdot \frac{1}{2}\Big((\varphi_A - \varphi_\sigma) \mathbf{N}_{A,\sigma} + (\varphi_{A^\star} - \varphi_{B^\star}) \mathbf{N}_{A,\sigma}^\star \Big).$$

To conclude, the required result follows by dividing and multiplying by $|\mathcal{D}_{A,\sigma}|$ each term of the sum, because we find the expression (2.7) (with the minus sign) in the last factor of the above identity. This yields the desired identification of $\Big[\!\Big[\mathrm{div}^{\mathcal{T}} \mathcal{F}^{\mathfrak{D}} \, , \, \varphi^{\mathcal{T}} \Big]\!\Big]_{\mathcal{T}} = \frac{1}{2}(X + Y + Z)$ with $\Big\{\!\Big\{ \mathcal{F}^{\mathfrak{D}} \, , \, -\nabla^{\mathfrak{D}} \varphi^{\overline{\mathcal{T}}} \Big\}\!\Big\}_{\mathfrak{D}}$. □

Calculations analogous to the Discrete Duality feature also permit to ascertain the weak (dual) consistency of the NDD discrete divergence operator. Recall that the projection operator $\mathbb{P}^{\mathcal{T}}$ of smooth functions on the mesh $\mathcal{T}$ was defined in Proposition 2.1. We further define the suitable projection $\mathbb{P}^{\mathfrak{D}}$ of smooth vector-fields, and claim the following.

Proposition 2.3. *Denote by $\mathbb{P}^{\mathfrak{D}}$ the following operator of projection of a smooth vector-field on $(\mathbb{R}^2)^{\mathfrak{D}}$: for $\psi \in C^\infty(\Omega;\mathbb{R}^2)$, $\mathbb{P}^{\mathfrak{D}}\psi$ is assigned the entries*

$$\psi_{\mathcal{D}_{A,\sigma}} := \frac{1}{|\sigma|}\int_\sigma \psi, \quad \forall \mathcal{D}_{A,\sigma} \in \mathfrak{D}.$$

The NDD discrete divergence operator $\operatorname{div}^{\mathcal{T}}$ is consistent in the weak-$\star$ $W^{-1,\infty}$ sense, that is, for each sequence $(\varphi^{\overline{\mathcal{T}}})_{\mathcal{T}}$, $\varphi^{\overline{\mathcal{T}}} \in \mathbb{R}_0^{\overline{\mathcal{T}}}$ with $\|\nabla^{\mathfrak{D}}\varphi^{\overline{\mathcal{T}}}\|_{L^1(\Omega)} \le const$,

$$\left[\!\!\left[\operatorname{div}^{\mathcal{T}}\left(\mathbb{P}^{\mathfrak{D}}\psi\right) - \mathbb{P}^{\mathcal{T}}\left(\operatorname{div}\psi\right), \varphi^{\mathcal{T}} \right]\!\!\right]_{\mathcal{T}} \to 0, \tag{2.13}$$

as the size $h^{\mathcal{T}}$ of $\mathcal{T}$ goes to zero, under the assumption (2.2) with some mesh-independent bound $\overline{\theta}$ of the regularity indicator $\theta^{\mathcal{D}}$.

Proof. First of all, observe that by definition, the field $\mathbb{P}^{\mathfrak{D}}\psi$ features conservative fluxes in the sense of Remark 2.3; we can denote by ψ_σ the common value $\psi_{\mathcal{D}_{A,\sigma}} = \psi_{\mathcal{D}_{B,\sigma}}$ where $\sigma \in \mathcal{E}_A \cap \mathcal{E}_B$. For this reason, the entries of $\mathbb{P}^{\mathcal{T}}\left(\operatorname{div}\psi\right)$ can be written in a way mimicking the definition of the discrete divergence operator. To be specific, in addition to the values $\psi_\sigma = \frac{1}{|\sigma|}\int_\sigma \psi$ introduced hereabove, we introduce

$$\psi^\star_{A,\sigma} := \frac{1}{|\sigma^\star_{A,\sigma}|}\int_{\sigma^\star_{A,\sigma}} \psi,$$

where we recall that, given $A \in \mathfrak{M}$, $\sigma \in \mathcal{E}_A$, we denote by $\sigma^\star_{A,\sigma}$ the dual interface contained in the diamond $\mathcal{D}_{A,\sigma}$. Then by the definition of $\mathbb{P}^{\mathcal{T}}$ in Proposition 2.1 and by the Green-Gauss integration-by-parts formula, for $A \in \mathfrak{M}$, $A^\star \in \mathfrak{M}^\star$ there holds

$$\mathbb{P}^{\mathcal{T}}\left(\operatorname{div}\psi\right)|_A = \frac{1}{|A|}\sum_{\sigma\in\mathcal{E}_A} \psi_\sigma \cdot \mathbf{N}_{A,\sigma},$$

in which we recognize $\operatorname{div}_A(\mathbb{P}^{\mathfrak{D}}\psi)$. The analogous calculation for the dual components of $\mathbb{P}^{\mathcal{T}}\left(\operatorname{div}\psi\right)$ leads to

$$\begin{aligned}
\mathbb{P}^{\mathcal{T}}\left(\operatorname{div}\psi\right)|_{A^\star} &= \frac{1}{|A^\star|}\sum_{A\in\mathfrak{M}_{A^\star}}\sum_{\substack{\sigma\in\mathcal{E}_A\\ A^\star\in\nu_\sigma}} \psi^\star_{A,\sigma}\cdot\mathbf{N}^{A^\star}_{A,\sigma} \\
&= \frac{1}{|A^\star|}\sum_{A\in\mathfrak{M}_{A^\star}}\sum_{\substack{\sigma\in\mathcal{E}_A\\ A^\star\in\nu_\sigma}} \left(\psi^\star_{A,\sigma}\cdot\mathbf{N}^{A^\star}_{A,\sigma} - \frac{1}{2}\psi_\sigma\cdot\mathbf{N}_{A,\sigma}\right) \\
&= \frac{1}{|A^\star|}\sum_{A\in\mathfrak{M}_{A^\star}}\sum_{\substack{\sigma\in\mathcal{E}_A\\ A^\star\in\nu_\sigma}} (\psi^\star_{A,\sigma}-\psi_\sigma)\cdot\mathbf{N}^{A^\star}_{A,\sigma} + \frac{1}{|A^\star|}\sum_{A\in\mathfrak{M}_{A^\star}}\sum_{\substack{\sigma\in\mathcal{E}_A\\ A^\star\in\nu_\sigma}} \psi_\sigma\cdot\widetilde{\mathbf{N}^{A^\star}_{A,\sigma}}.
\end{aligned}$$

Above, the second identity is due to (2.10) and to the aforementioned conservativity of the fluxes (Remark 2.3), i.e., to the cancellation of the terms $\psi_\sigma\cdot\mathbf{N}_{A,\sigma}$, $\psi_\sigma\cdot\mathbf{N}_{B,\sigma}$ coming from A, B such that $\sigma = A|B$; and the last equality is due to the definition (2.10) of $\widetilde{\mathbf{N}^{A^\star}_{A,\sigma}}$, upon adding and subtracting $\psi_\sigma\cdot\mathbf{N}^{A^\star}_{A,\sigma}$. Now, recalling the definition of $\mathbb{P}^{\mathfrak{D}}$ and of $\operatorname{div}_{A^\star}$, in the last term of the right-hand side of the above identity we recognize $\operatorname{div}_{A^\star}(\mathbb{P}^{\mathfrak{D}}\psi)$. Therefore, canceling the identical terms we find

$$\begin{aligned}
\left[\!\!\left[\operatorname{div}^{\mathcal{T}}\left(\mathbb{P}^{\mathfrak{D}}\psi\right) - \mathbb{P}^{\mathcal{T}}\left(\operatorname{div}\psi\right), \phi^{\mathcal{T}} \right]\!\!\right] &= \frac{1}{2}\sum_{A^\star\in\mathfrak{M}^\star}\sum_{A\in\mathfrak{M}_{A^\star}}\sum_{\substack{\sigma\in\mathcal{E}_A\\ A^\star\in\nu_\sigma}} \varphi_{A^\star}\,(\psi^\star_{A,\sigma}-\psi_\sigma)\cdot\mathbf{N}^{A^\star}_{A,\sigma} \\
&= \frac{1}{2}\sum_{A\in\mathfrak{M}}\sum_{\sigma\in\mathcal{E}_A} (\varphi_{A^\star_\sigma}-\varphi_{B^\star_\sigma})(\psi^\star_{A,\sigma}-\psi_\sigma)\cdot\mathbf{N}^\star_{A,\sigma},
\end{aligned}$$

where we used the conservativity of the dual fluxes while gathering the terms per diamond. Further, $\psi^\star_{A,\sigma} - \psi_\sigma$ is order one small with respect to the size $h^{\mathcal{T}}$ of the mesh, because ψ is smooth. Dividing and multiplying by $|\sigma|$, having in mind that $\left|\frac{\varphi_{B^\star_\sigma} - \varphi_{A^\star_\sigma}}{|\sigma|}\right| \le const\, |\nabla_{\mathcal{D}_{A,\sigma}} \varphi^{\overline{\mathcal{T}}}|$ with the constant that only depends on the regularity bound $\overline{\theta}$ of the mesh (see (2.6)), we deduce the required claim. □

3 Nodal discrete duality scheme and its properties

In this section, we propose and present the nodal discrete duality discretization for the nonlinear elliptic problem (1.1) and sketch some of its crucial mathematical properties.

3.1 The nonlinear NDD scheme

We start by prescribing the discretization of the space dependence of the flux $\boldsymbol{\alpha}$ in (1.1). In general, we can use the diamond averages

$$\boldsymbol{\alpha}_{\mathcal{D}}(\zeta) = \frac{1}{|\mathcal{D}|} \int_{\mathcal{D}} \boldsymbol{\alpha}(x,\zeta)\,\mathrm{d}x, \quad \forall \zeta \in \mathbb{R}^2, \tag{3.1}$$

for $\mathcal{D} \in \mathfrak{D}$. If $\boldsymbol{\alpha}$ is continuous with respect to its first argument, we can also use the more practical discretization $\boldsymbol{\alpha}_{\mathcal{D}}(\zeta) = \boldsymbol{\alpha}(x_A, \zeta)$ for $\mathcal{D} = \mathcal{D}_{A,\sigma}$.

Then, $\zeta = \nabla u$ in the continuous problem is substituted with the discrete gradient $\nabla^{\mathfrak{D}}$. This leads to the natural per-diamond definition of the discrete flux:

$$\boldsymbol{\alpha}^{\mathfrak{D}}\big(\nabla^{\mathfrak{D}} u^{\overline{\mathcal{T}}}\big) = \Big(\boldsymbol{\alpha}_{\mathcal{D}}\big(\nabla_{\mathcal{D}} u^{\overline{\mathcal{T}}}\big)\Big)_{\mathcal{D}\in\mathfrak{D}} \in (\mathbb{R}^2)^{\mathfrak{D}}. \tag{3.2}$$

Further, the source term f is approximated by $f^{\mathcal{T}} := \mathbb{P}^{\mathcal{T}} f$, i.e.,

$$f^{\mathcal{T}} = \Big((f_A)_{A\in\mathfrak{M}}, (f_{A^\star})_{A^\star\in\mathfrak{M}^\star}\Big), \ \text{ with } \ f_K := \frac{1}{|K|}\int_K f(x)\,\mathrm{d}x, \ \forall K \in \mathfrak{M}\cup\mathfrak{M}^\star \tag{3.3}$$

(as usual, for piecewise continuous f one can replace f_K by $f(x_K)$). Finally, the nodal discrete scheme for (1.1) consists of the nonlinear system of algebraic equations

$$\begin{cases} -\mathrm{div}_A\ \boldsymbol{\alpha}^{\mathfrak{D}}\big(\nabla^{\mathfrak{D}} u^{\overline{\mathcal{T}}}\big) = f_A, \quad \forall A \in \mathfrak{M}, \\ -\mathrm{div}_{A^\star}\ \boldsymbol{\alpha}^{\mathfrak{D}}\big(\nabla^{\mathfrak{D}} u^{\overline{\mathcal{T}}}\big) = f_{A^\star}, \quad \forall A^\star \in \mathfrak{M}^\star, \\ u_{A^\star} = 0, \quad \forall A^\star \in \partial\mathfrak{M}^\star \end{cases} \tag{3.4}$$

or, in a fully concise form,

$$\text{find } u^{\mathcal{T}} \in \mathbb{R}^{\mathcal{T}}_0 \text{ such that } \quad -\mathrm{div}^{\mathcal{T}}\, \boldsymbol{\alpha}^{\mathfrak{D}}(\nabla^{\mathfrak{D}} u^{\overline{\mathcal{T}}}) = \mathbb{P}^{\mathcal{T}} f. \tag{3.5}$$

Remark 3.1. *Note that the abstract form* (3.5) *encoding the system* (3.4) *is compact and suitable for the analysis, but it is inadequate in practice. For the implementation, we rather prefer the equivalent formulation close to the standard DDFV formalism using the straightforwardly defined primal and dual fluxes:*

$$\begin{cases} \displaystyle\sum_{\sigma\in\mathcal{E}_A} F_{A,\sigma}(u^{\mathcal{T}}) = |A|\, f_A, \quad \forall A \in \mathfrak{M}, \\ \displaystyle\sum_{A\in\mathfrak{M}_{A^\star}} \sum_{\substack{\sigma\in\mathcal{E}_A \\ A^\star\in\nu_\sigma}} \Big(F^{A^\star}_{A,\sigma}(u^{\mathcal{T}}) - \frac{1}{2} F_{A,\sigma}(u^{\mathcal{T}})\Big) = |A^\star|\, f_{A^\star}, \quad \forall A^\star \in \mathfrak{M}^\star, \\ u_{A^\star} = 0, \quad \forall A^\star \in \partial\mathfrak{M}^\star, \end{cases} \tag{3.6}$$

where the fluxes $F_{A,\sigma}(u^{\mathcal{T}}), F^\star_{A^\star,\sigma}(u^{\mathcal{T}})$ are expressed by

$$F_{A,\sigma}(u^{\mathcal{T}}) = -\,|\sigma|\, \boldsymbol{\alpha}_{\mathcal{D}_{A,\sigma}}(\nabla_{\mathcal{D}_{A,\sigma}} u^{\mathcal{T}}) \cdot \mathbf{n}_{A,\sigma}, \tag{3.7}$$

$$F^{A^\star}_{A,\sigma}(u^{\mathcal{T}}) = -\,\big|\sigma^\star_{A,\sigma}\big|\, \boldsymbol{\alpha}_{\mathcal{D}_{A,\sigma}}(\nabla_{\mathcal{D}_{A,\sigma}} u^{\overline{\mathcal{T}}}) \cdot \mathbf{n}^{A^\star}_{A,\sigma}. \tag{3.8}$$

Remark 3.2. *Let us highlight the fact that the nodal discrete duality scheme does not possess the standard finite volume structure, for the two following reasons.*

The first one is that conservation of the primal fluxes is not encoded into the scheme, see Remark 2.3. The lack of conservativity can be seen as the price to pay for the elimination of the node DOFs, see Section 3.4 below[3]
This is due to the fact that, in the NDD construction of the discrete gradient, we do not take finite differences across the primal interfaces (the cell DOF is connected only to its surrounding vertices, which facilitates its elimination at a low numerical cost).

On the other hand, the discrete divergence operator does not possess the straightforward interpretation in terms of the Green-Gauss theorem, unlike the usual Finite Volume discrete divergence operators. Indeed, in the calculation of the divergence associated to the dual cells, the dual weighted normal $\widetilde{\mathbf{N}_{A,\sigma}^{A^\star}}$ *is deviated from the standard DDFV dual weighted normal* $\mathbf{N}_{A,\sigma}^{A^\star}$*. It can be noted that the correction imposed via* (2.10) *is precisely a way to take into account the non-conservativity of the primal fluxes, see Remark 2.3.*

In this context, we stress two facts, to claim that the deviation of the NDD construction from the Finite Volume guidelines does not have dramatic consequences on the key scheme properties underlying its analysis. First, the discrete divergence operator retains the weak consistency property typical of Finite Volume schemes (Proposition 2.3); note that the lack of a strong consistency is not unusual for Finite Volume schemes (cf. [20, Rem. 1.3]). Second, the Discrete Duality feature (Proposition 2.2) accounts for a global conservativity property of NDD, even if the local conservativity for the primal fluxes is not encoded in the NDD scheme.

3.2 A priori estimates on discrete solutions

The developed scheme guarantees a discrete counterpart of the a priori estimates independently of the mesh size. To express these estimates, we equip $\mathbb{R}_0^{\mathcal{T}}$ with the L^p-like norm $\|\cdot\|_{0,p}$ and with the $W_0^{1,p}$-like semi-norm $\|\cdot\|_{1,p}$ defined by

$$\left\|v^{\mathcal{T}}\right\|_{0,p} = \left(\frac{1}{2}\sum_{A\in\mathfrak{M}} |A|\,|v_A|^p + \frac{1}{2}\sum_{A^\star\in\overline{\mathfrak{M}^\star}} |A^\star|\,|v_{A^\star}|^p\right)^{1/p}, \quad \left\|v^{\mathcal{T}}\right\|_{1,p} = \left(\sum_{\mathcal{D}\in\mathfrak{D}} |\mathcal{D}|\left|\nabla_{\mathcal{D}}\, v^{\overline{\mathcal{T}}}\right|^p\right)^{1/p}.$$

First, we recall the discrete Poincaré's inequality, which is of great importance for the analysis. One of its consequences is that the semi-norm $\|\cdot\|_{1,p}$ becomes a norm on $\mathbb{R}_0^{\mathcal{T}}$.

Lemma 3.1. *The exists a positive constant* C_0 *depending only on the exponent* p*, the diameter of* Ω *and the mesh regularity such that*

$$\left\|u^{\mathcal{T}}\right\|_{0,p} \le C_0 \left\|u^{\mathcal{T}}\right\|_{1,p}, \quad \forall u^{\mathcal{T}} \in \mathbb{R}_0^{\mathcal{T}}.$$

The proof can be inferred from the corresponding DDFV proof ([8]).

Second, the equations of the scheme can be reformulated in a concise variational form[4] by means of Proposition 2.2:

$$\left\{\!\!\left\{\boldsymbol{\alpha}^{\mathfrak{D}}\left(\nabla^{\mathfrak{D}} u^{\overline{\mathcal{T}}}\right),\, \nabla^{\mathfrak{D}}\varphi^{\overline{\mathcal{T}}}\right\}\!\!\right\}_{\mathcal{D}} = \left[\!\!\left[f^{\mathcal{T}}, \varphi^{\mathcal{T}}\right]\!\!\right]_{\mathcal{T}}, \quad \forall \varphi^{\mathcal{T}} \in \mathbb{R}_0^{\mathcal{T}}. \tag{3.9}$$

This viewpoint, combined with the Poincaré's inequality, readily yields to discrete counterpart of the "energy" estimates for the variational formulation of the continuous problem.

[3] It is worth mentioning that the VAG (Vertex Approximate Gradient) scheme [12, 13, 24] also makes use of the $\mathbb{P}_1$ finite elements gradient on the sub-mesh to define the generalized fluxes (cf. Remark 2.2. The appealing feature of the NDD scheme is that the flux $F_{A,\sigma}(u^{\mathcal{T}})$ requires unknowns including only the DOFs located at the vertices x_A, $x_{A_\sigma^\star}$, $x_{B_\sigma^\star}$, which are the vertices of the NDD diamond $\mathcal{D}_{A,\sigma}$; while in the context of the VAG scheme, the expression of the flux involves all the DOFs attached to the vertices of A.

[4] As in [8], it can be inferred from Proposition 2.2 that, in the case where $\boldsymbol{\alpha}(x,\cdot)$ derives from a potential, the NDD scheme encodes the minimization, over the discrete space $\mathbb{R}_0^{\mathcal{T}}$, of a discrete energy functional resembling closely the continuous energy functional.

Proposition 3.1. *Let $u^{\mathcal{T}} \in \mathbb{R}_0^{\mathcal{T}}$ be a solution of the numerical scheme* (3.2)–(3.6)*. There exist positive constants C_1, C_2, C_3 depending only on the data specified in* ***(H_1)-(H_2)****, Ω and the mesh regularity such that*

$$\left\{\boldsymbol{\alpha}^{\mathfrak{D}}\left(\nabla^{\mathfrak{D}} u^{\overline{\mathcal{T}}}\right), \nabla^{\mathfrak{D}} u^{\overline{\mathcal{T}}}\right\}_{\mathfrak{D}} \leq C_1, \tag{3.10}$$

$$\left\|u^{\mathcal{T}}\right\|_{1,p} \leq C_2, \tag{3.11}$$

$$\|\boldsymbol{\alpha}^{\mathfrak{D}}\left(\nabla^{\mathfrak{D}} u^{\overline{\mathcal{T}}}\right)\|_{L^{p'}(\Omega)}^{p'} \leq C_3. \tag{3.12}$$

Proof. Using the equations of the numerical scheme (3.4) under the form (3.9) with the discrete test function $\varphi^{\mathcal{T}} = u^{\mathcal{T}}$ entails

$$E_l := \left\{\boldsymbol{\alpha}^{\mathfrak{D}}\left(\nabla^{\mathfrak{D}} u^{\overline{\mathcal{T}}}\right), \nabla^{\mathfrak{D}} u^{\overline{\mathcal{T}}}\right\}_{\mathfrak{D}} = \left[\!\left[f^{\mathcal{T}}, u^{\mathcal{T}}\right]\!\right]_{\mathcal{T}} := E_r.$$

Next, the Hölder, Poincaré and Young inequalities imply

$$|E_r| \leq \widetilde{C}_1 + \frac{C_{\boldsymbol{\alpha}}}{p}\left\|u^{\mathcal{T}}\right\|_{1,p}^p, \quad \widetilde{C}_1 = \frac{C_0^{p'}\,\|f\|_{L^{p'}(\Omega)}^{p'}}{p' C_{\boldsymbol{\alpha}}^{\frac{p'}{p}}}.$$

Now, introduce the coercivity constant of $\boldsymbol{\alpha}$ specified in (1.2a), where $\zeta = \nabla_{\mathcal{D}_{A,\sigma}} u^{\overline{\mathcal{T}}}$, integrate on $\mathcal{D}_{A,\sigma}$, and sum over $\sigma \in \mathcal{E}_A$ together with $A \in \mathfrak{M}$ to deduce

$$C_{\boldsymbol{\alpha}}\left\|u^{\mathcal{T}}\right\|_{1,p}^p \leq \|m_0\|_{L^1(\Omega)} + |E_l|.$$

Therefore, $|E_r|$ is estimated by

$$|E_r| \leq \widetilde{C}_1 + \frac{1}{p}\|m_0\|_{L^1(\Omega)} + \frac{1}{p}|E_l|.$$

As a result, one gets

$$|E_l| \leq p'\widetilde{C}_1 + \frac{p'}{p}\|m_0\|_{L^1(\Omega)} \quad \text{and} \quad \left\|u^{\mathcal{T}}\right\|_{1,p} \leq \left(\frac{p'\widetilde{C}_1}{C_{\boldsymbol{\alpha}}} + \frac{p+p'}{pC_{\boldsymbol{\alpha}}}\|m_0\|_{L^1(\Omega)}\right)^{1/p}.$$

Finally, use (1.2b) to deduce a bound of the form (3.12). The proof is then concluded. □

3.3 Existence and uniqueness of the approximate solution

In this paragraph, we demonstrate that the NDD scheme (3.4) enjoys existence and uniqueness of a discrete solution. The existence proof exploits the following corollary of the Brouwer fixed-point theorem ([31, Lem. 4.3],[23, p. 493]) that permits to assert that some vector fields possess zeros.

Lemma 3.2. *Let $\Phi : \mathbb{R}^n \to \mathbb{R}^n$ be a continuous function. Assume that for some $r > 0$,*

$$\forall \boldsymbol{x} \text{ such that } |\boldsymbol{x}| = r, \qquad \Phi(\boldsymbol{x}) \cdot \boldsymbol{x} \geq 0.$$

Then, there exists $\boldsymbol{x}^\star \in \mathbb{R}^n$, with $|\boldsymbol{x}^\star| \leq r$, such that $\Phi(\boldsymbol{x}^\star) = 0$.

The solvability of our scheme is a consequence of the *a priori* estimates of Proposition 3.1 and of Lemma 3.2, while the uniqueness is a result of the scheme monotonicity. Also note that in the linear case (cf. Section 3.4 for details on this case) the non-constructive existence proof can be replaced by the elementary and constructive linear algebra arguments. To sum up, we have

Proposition 3.2. *The nonlinear algebraic system that expresses the NDD scheme* (3.4) *admits a unique solution.*

Let us just highlight that in practice, (3.4) is implemented under the form (3.6)–(3.8) via the Newton method, where the node unknowns are eliminated at each Newton iteration step (see Sections 3.4,6 for details).

Proof. We divide the proof into two steps.
• *Existence.* Fix $n = \#(\mathfrak{M} \cup \mathfrak{M}^\star)$. Define $\Phi : \mathbb{R}^n \to \mathbb{R}^n$ such that for each $u^{\mathcal{T}}$ we associate a vector $\Phi(u^{\mathcal{T}})$ whose components write

$$\begin{cases} \Phi(u^{\mathcal{T}})_{|A} = -|A| \operatorname{div}_A \boldsymbol{\alpha}^{\mathfrak{D}}\left(\nabla^{\mathfrak{D}} u^{\overline{\mathcal{T}}}\right) - |A| f_A, \quad \forall A \in \mathfrak{M}, \\ \Phi(u^{\mathcal{T}})_{|A^\star} = -|A^\star| \operatorname{div}_{A^\star} \boldsymbol{\alpha}^{\mathfrak{D}}\left(\nabla^{\mathfrak{D}} u^{\overline{\mathcal{T}}}\right) - |A^\star| f_A^\star, \quad \forall A^\star \in \mathfrak{M}^\star. \end{cases}$$

The values of $u^{\mathcal{T}}$ at the boundary cells $\partial\mathfrak{M}^\star$ are set to 0; thus $u^{\mathcal{T}}$ is assimilated to an element of $\mathbb{R}_0^{\mathcal{T}}$. If $u^{\mathcal{T}}$ satisfies $\Phi(u^{\mathcal{T}}) = 0$, then it is a solution to the numerical scheme (3.4). The continuity of Φ is inherited from the continuity of $\boldsymbol{\alpha}$ with respect to its second argument. Thanks to the estimation (3.2) and Poincaré's inequality we obtain

$$\Phi(u^{\mathcal{T}}) \cdot u^{\mathcal{T}} \geq \frac{C_{\boldsymbol{\alpha}}}{C_0^p} \left\|u^{\mathcal{T}}\right\|_{0,p}^p - \|m_0\|_{L^1(\Omega)}.$$

The function $u^{\mathcal{T}} \to \left\|u^{\mathcal{T}}\right\|_{0,p}$ is a norm on $\mathbb{R}^n$. Set $r = \left(C_0^p \|m_0\|_{L^1(\Omega)} / C_{\boldsymbol{\alpha}} + 1\right)^{1/p}$. As a result

$$\Phi(u^{\mathcal{T}}) \cdot u^{\mathcal{T}} \geq 0, \quad \forall u^{\mathcal{T}} : \left\|u^{\mathcal{T}}\right\|_{0,p} = r.$$

Thereby, Lemma 3.2 ensures the existence of at least one solution $u^{\mathcal{T}}$ solving the NDD numerical scheme (3.4).
• *Uniqueness.* Suppose that there exists another solution to the scheme denoted by $v^{\mathcal{T}}$. Using Proposition 2.2, we find

$$\sum_{A \in \mathfrak{M}} \sum_{\sigma \in \mathcal{E}_A} |\mathcal{D}_{A,\sigma}| \left(\boldsymbol{\alpha}_{\mathcal{D}_{A,\sigma}}(\nabla_{\mathcal{D}_{A,\sigma}} u^{\overline{\mathcal{T}}}) - \boldsymbol{\alpha}_{\mathcal{D}_{A,\sigma}}(\nabla_{\mathcal{D}_{A,\sigma}} v^{\overline{\mathcal{T}}})\right) \cdot \left(\nabla_{\mathcal{D}_{A,\sigma}} u^{\overline{\mathcal{T}}} - \nabla_{\mathcal{D}_{A,\sigma}} v^{\overline{\mathcal{T}}}\right) = 0. \tag{3.13}$$

The strict monotonicity of $\boldsymbol{\alpha}$ prescribed by (1.2c) enforces that $\nabla_{\mathcal{D}_{A,\sigma}}(u^{\overline{\mathcal{T}}} - v^{\overline{\mathcal{T}}}) = 0$, for all $A \in \mathfrak{M}$ and all $\sigma \in \mathcal{E}_A$. As consequence of Poincaré's inequality, the both solutions $u^{\mathcal{T}}$ and $v^{\mathcal{T}}$ coincide, which finishes the proof. □

3.4 Local elimination of cell unknowns

While the construction of the NDD scheme calls upon both the node and the cell unknowns, in practice after a computationally inexpensive algebraic procedure it reduces to a nodal scheme, which is reflected in its name (NDD, for *Nodal Discrete Duality*). Indeed, let us sketch how the cell unknowns are eliminated; let us detail the case where the flux $\boldsymbol{\alpha}$ in problem (1.1) is linear, taking the form $\boldsymbol{\alpha}(\cdot, \zeta) = \Lambda(\cdot)\zeta$. The numerical scheme becomes linear and can be recast under the matrix form $\mathbf{A}u^{\mathcal{T}} = b^{\mathcal{T}}$. More precisely, it offers the block structure

$$\begin{pmatrix} \mathbf{A_{11}} & \mathbf{A_{12}} \\ \mathbf{A_{21}} & \mathbf{A_{22}} \end{pmatrix} \begin{pmatrix} u^{\mathfrak{M}^\star} \\ u^{\mathfrak{M}} \end{pmatrix} = \begin{pmatrix} \boldsymbol{b}^{\mathfrak{M}^\star} \\ \boldsymbol{b}^{\mathfrak{M}} \end{pmatrix},$$

The block $\mathbf{A_{11}}$ gathers the vertex contributions and it is of size $\#\mathfrak{M}^\star$. Similarly, $\mathbf{A_{22}}$ contains the cell contributions. Its size is $\#\mathfrak{M}$. The two remaining blocks, i.e., $\mathbf{A_{12}}, \mathbf{A_{21}}$, account for the interaction between the vertices together with cells and vice-versa. A key feature in $\boldsymbol{A}$ is that the block $\mathbf{A_{22}}$ is an invertible diagonal matrix. Consequently, the Schur complement is easily computed and the final system to be solved reduces to

$$\left(\mathbf{A_{11}} - \mathbf{A_{12}}\mathbf{A_{22}^{-1}}\mathbf{A_{21}}\right) u^{\mathfrak{M}^\star} = \boldsymbol{b}^{\mathfrak{M}^\star} - \mathbf{A_{12}}\mathbf{A_{22}^{-1}}\boldsymbol{b}^{\mathfrak{M}},$$

where we stress that only the vertex unknowns are involved in the resolution process. The cell unknowns are eliminated without fill-in and they can be updated using the simple relationship

$$u^{\mathfrak{M}} = \mathbf{A_{22}^{-1}}\left(\boldsymbol{b}^{\mathfrak{M}^\star} - \mathbf{A_{21}} u^{\mathfrak{M}^\star}\right).$$

We emphasize that in the nonlinear case, the elimination process is performed at the level of the Newton solver.

4 Convergence analysis for NDD discretization

In this section we provide a succinct account on the convergence analysis of the NDD scheme for the problem (1.1). The argumentation follows closely the analysis of [8] (see also [2]) for DDFV scheme for the same class of PDEs. We highlight only the essential differences related to the issues discussed in Remark 3.2 (the noticeable differences between NDD and Finite Volume schemes) and the advantages offered by NDD:

- the NDD scheme does not require penalization of the difference between the primal and the dual components of the solution, see Remark 4.1;
- the NDD scheme does not require adaptation to handle efficiently diffusion tensors that may have discontinuities aligned with primal interfaces, see Remark 4.2(ii).

In contrast to [8], we outline only the basic convergence analysis based upon compactness; we refer to Remark 4.2(i) for a brief discussion on error analysis.

First, let us provide the NDD version of the discrete $W_0^{1,p}$ compactness result.

Proposition 4.1. *Let $(\mathcal{T}_k)_{k\in\mathbb{N}}$ be a sequence of discretizations to the domain Ω such that $h^{\mathcal{T}_k}$ tends to 0 as k goes to $+\infty$ and their regularity parameters $(\theta^{\mathcal{D}})_{\mathcal{D}\in\mathfrak{D}_k,k\in\mathbb{N}}$ are uniformly bounded by some constant $\overline{\theta}$, see (2.2). Let $(u^{\mathcal{T}_k})_{k\in\mathbb{N}}$ be a sequence of associated discrete functions assuming zero values in boundary cells, i.e., $u^{\mathcal{T}_k}\in\mathbb{R}_0^{\mathcal{T}_k}$. Assume that $\left\|u^{\mathcal{T}_k}\right\|_{1,p}$ is uniformly bounded.*

Then there exists $u\in W_0^{1,p}(\Omega)$ and a (not relabeled) subsequence of meshes such that

$$\begin{array}{lll} u^{\mathfrak{M}_k}, u^{\overline{\mathfrak{M}^\star}_k} & \xrightarrow[k\to+\infty]{} u & \text{strongly in } L^p(\Omega), \\ \nabla^{\mathfrak{D}_k} u^{\overline{\mathcal{T}}_k} & \xrightarrow[k\to+\infty]{} \nabla u & \text{weakly in } L^p(\Omega;\mathbb{R}^2). \end{array} \tag{4.1}$$

Remark 4.1. *Let us stress that in the DDFV context, the typical compactness result differs from the above ones in its conclusions, because $u^{\mathfrak{M}_k}, u^{\overline{\mathfrak{M}^\star}_k}$ may not converge to the same limit. Actually, in the DDFV context u is identified to the strong limit of $u^{\mathcal{T}_k}=\frac{1}{2}\left(u^{\mathfrak{M}_k}+u^{\overline{\mathfrak{M}^\star}_k}\right)$, see (2.4). While in simpler situations including problem (1.1) it is possible to show that the discrete solution components $u^{\mathfrak{M}_k}, u^{\overline{\mathfrak{M}^\star}_k}$ do converge to the same limit ([8]), for more complex PDEs the hint of double mesh penalization was developed ([5, 2]) in order to guarantee that $u^{\mathfrak{M}_k}-u^{\overline{\mathfrak{M}^\star}_k}$ tends to zero in the appropriate strong sense, as $k\to\infty$.*

The above result demonstrates that in the NDD case, the identification between the strong limits of $u^{\mathfrak{M}_k}, u^{\overline{\mathfrak{M}^\star}_k}$ is automatic, it stems from the nature of the NDD discrete gradient and essentially relies upon Remark 2.2.

Proof. (sketched) First, note that the uniform bound on $\left\|u^{\mathcal{T}_k}\right\|_{1,p}$ means the uniform bound on the functions $\nabla^{\mathfrak{D}_k}u^{\overline{\mathcal{T}}_h}$ in $L^p(\Omega;\mathbb{R}^2)$; moreover, the Poincaré inequality of Lemma 3.1 and the definition of $\|\cdot\|_{0,p}$ implies the $L^p(\Omega)$ bound on both $u^{\mathfrak{M}_k}$ and $u^{\overline{\mathfrak{M}^\star}_k}$. The relative compactness in the weak topology of bounded in L^p sets yields the weak convergence (up to a subsequence) of $\nabla^{\mathfrak{D}_k}u^{\overline{\mathcal{T}}_k}$ to some limit that we denote χ, $\chi\in L^p(\Omega;\mathbb{R}^2)$, and the weak convergence (up to a further subsequence) of $u^{\mathcal{T}_k}=\frac{1}{2}(u^{\mathfrak{M}_k}+u^{\overline{\mathfrak{M}^\star}_k})$ to some limit that we denote u, $u\in L^p(\Omega)$. Then, as in [8], we identify χ to the distributional gradient of u by showing that

$$\forall\psi\in C^\infty(\Omega;\mathbb{R}^2)\quad \int_\Omega \chi(x)\cdot\psi(x)\,\mathrm{d}x=-\int_\Omega \operatorname{div}\psi(x)u(x)\,\mathrm{d}x. \tag{4.2}$$

This shows in passing that u actually belongs to $W_0^{1,p}(\Omega)$. To this aim, we start with the discrete duality identity (2.11) written for the discrete vector-function $\mathbb{P}^{\mathfrak{D}_k}\psi\in(\mathbb{R}^2)^{\mathfrak{D}_k}$ (the projection operator $\mathbb{P}^{\mathfrak{D}}$ being defined in Proposition 2.3) and the discrete function $u^{\overline{\mathcal{T}}_k}\in\mathbb{R}_0^{\overline{\mathcal{T}}_k}$. Then we pass to the limit, as $k\to\infty$, using the weak consistency property for $\operatorname{div}^{\mathcal{T}_k}$, as stated in Proposition 2.3, and the obvious strong $L^{p'}(\Omega;\mathbb{R}^2)$ convergence of $\mathbb{P}^{\mathfrak{D}_k}\psi$ to ψ. At the limit, we find (4.2).

Now we demonstrate the appealing feature of the NDD scheme, in comparison to DDFV schemes, namely that u is not only the limit of the average of the reconstructions $u^{\mathfrak{M}_k}$ (on the primal mesh) and $u^{\overline{\mathfrak{M}^\star}_k}$ (on the dual mesh), but the two reconstructions have a common limit. To this end, we split Ω into the disjoint

(up to a set of zero two-dimensional Lebesgue measure) union of polygons $A\cap A^\star$, $A\in\mathfrak{M}_k$, $A^\star\in\overline{\mathfrak{M}^\star}_k$; each of these polygons has the diameter smaller that $h^{\mathcal{T}_k}$. The function $x\mapsto u^{\mathfrak{M}_k}(x)-u^{\overline{\mathfrak{M}^\star}_k}(x)$ on Ω is constant on each of these polygons. From the observation of Remark 2.2, from the definition of the reconstructions $u^{\mathfrak{M}_k}, u^{\overline{\mathfrak{M}^\star}_k}$ and $\nabla^{\mathfrak{D}_k}u^{\overline{\mathcal{T}}_k}$ on Ω we readily deduce

$$\forall x\in A\cap A^\star\quad |u^{\mathfrak{M}_k}(x)-u^{\overline{\mathfrak{M}^\star}_k}(x)|=|u_A-u_A^\star|\le h^{\mathcal{T}_k}\min\Big\{|\nabla_{\mathcal{D}_{A,\sigma'}}u^{\overline{\mathcal{T}}_k}|,|\nabla_{\mathcal{D}_{A,\sigma''}}u^{\overline{\mathcal{T}}_k}|\Big\},$$

where σ',σ'' are the two edges of A having $x_{A^\star}$ as a vertex. Whence we find

$$\|u^{\mathfrak{M}_k}-u^{\overline{\mathfrak{M}^\star}_k}\|_{L^p(\Omega)}\le h^{\mathcal{T}_k}\|\nabla^{\mathfrak{D}_k}u^{\overline{\mathcal{T}}_k}\|_{L^p(\Omega;\mathbb{R}^2)}=h^{\mathcal{T}_k}\left\|u^{\mathcal{T}_k}\right\|_{1,p},$$

so that from the uniform discrete $W_0^{1,p}$ bound on $u^{\mathcal{T}_k}$ we deduce that $u^{\mathfrak{M}_k}$, $u^{\overline{\mathfrak{M}^\star}_k}$ have the same weak $L^p(\Omega)$ limit (up to a subsequence, as stated above).

Finally, we point out that the weak L^p convergence of $u^{\mathfrak{M}_k}, u^{\overline{\mathfrak{M}^\star}_k}$ to u can be upgraded to the strong convergence. The latter fact relies on the strong L^p compactness of $(u^{\mathfrak{M}_k})_{k\in\mathbb{N}}$,$(u^{\overline{\mathfrak{M}^\star}_k})_{k\in\mathbb{N}}$ due to the uniform control of their translates. Indeed, it follows from the analysis present, e.g., in [8, 2, 34] that

$$\|u^{\mathfrak{M}_k}(\cdot+\boldsymbol{\tau})-u^{\mathfrak{M}_k}\|_{L^p(\mathbb{R}^2)}\le C(|\boldsymbol{\tau}|+h^{\mathcal{T}_k})\left\|u^{\mathcal{T}_k}\right\|_{1,p},\quad\forall\boldsymbol{\tau}\in\mathbb{R}^2 \tag{4.3}$$

and the same relation holds with $u^{\mathfrak{M}_k}$ replaced by $u^{\overline{\mathfrak{M}^\star}_k}$, with the constant C depending only on the exponent p and the mesh regularity. □

Now we are ready to state the convergence theorem for NDD discretizations of (1.1).

Theorem 4.1. *Assume that **($\boldsymbol{H}_1$)-($\boldsymbol{H}_2$)** are satisfied. Let $(\mathcal{T}_k)_{k\in\mathbb{N}}$ be a sequence of discretizations of the domain Ω such that $h^{\mathcal{T}_k}$ tends to 0 as k goes to $+\infty$ and their regularity constants $(\theta^{\mathcal{D}})_{\mathcal{D}\in\mathfrak{D}_k,k\in\mathbb{N}}$ are uniformly bounded by some constant $\overline{\theta}$, see* (2.2)*. Consider the sequence $(u^{\mathcal{T}_k})_{k\in\mathbb{N}}$ of the associated solutions to the scheme* (3.2)–(3.4)*. There exists $u\in W_0^{1,p}(\Omega)$ such that*

$$\begin{aligned}&u^{\mathcal{T}_k}\ \xrightarrow[k\to+\infty]{}\ u\quad&&\text{strongly in } L^p(\Omega),\\&\nabla^{\mathfrak{D}_k}u^{\overline{\mathcal{T}}_k}\ \xrightarrow[k\to+\infty]{}\ \nabla u\quad&&\text{strongly in } L^p(\Omega;\mathbb{R}^2).\end{aligned} \tag{4.4}$$

The limit u is the unique weak solution (in the sense of Definition 1.1) to the continuous model (1.1)*.*

Proof. The convergence claims - up to extraction of a subsequence, and with the weak convergence for the discrete gradients in the place of the strong one - stem from Proposition 4.1, having in mind the estimate (3.11). As soon as we prove that any such accumulation point u satisfies the weak formulation (1.4), by uniqueness and the standard *reductio ad absurdum* argument we will conclude that the extraction of a subsequence can be bypassed.

To check that u is a solution of (1.1) we will exploit the Minty-Browder argument [33], which is standard in the context of (1.1) ([30]). First, observe that estimate (3.12) yields the weak $L^{p'}(\Omega;\mathbb{R}^2)$ convergence (up to a further extraction of a subsequence, which we do not relabel) of the discrete fluxes $\boldsymbol{\alpha}^{\mathfrak{D}_k}\big(\nabla^{\mathfrak{D}_k}u^{\overline{\mathcal{T}}_k}\big)$ (identified in the usual way with an $\mathbb{R}^2$-valued function on Ω) to some limit that we denote Υ; it has to be shown that Υ coincides with $\boldsymbol{\alpha}(\cdot,\nabla u)$.

Take $\varphi\in\mathcal{C}_0^\infty(\Omega)$. Consider $\varphi^{\mathcal{T}_k}:=\mathbb{P}^{\mathcal{T}_k}\varphi\in\mathbb{R}_0^{\mathcal{T}_k}$, as defined in Proposition 2.1. Having in mind the definitions of $\boldsymbol{\alpha}^{\mathfrak{D}}$ and $f^{\mathcal{T}}$, taking this test function in the variational reformulation (3.9) yields

$$\int_\Omega\boldsymbol{\alpha}(x,\nabla^{\mathfrak{D}_k}u^{\overline{\mathcal{T}}_k})\cdot\nabla^{\mathfrak{D}_k}\mathbb{P}^{\overline{\mathcal{T}}_k}\varphi\,\mathrm{d}x=\int_\Omega f\,\mathbb{P}^{\mathcal{T}_k}\varphi\,\mathrm{d}x.$$

Owing to the smoothness of φ we readily have $\mathbb{P}^{\mathcal{T}_k}\varphi\to\varphi$ in $L^p(\Omega)$, moreover, we can apply Proposition 2.1 to get as well the strong $L^p(\Omega;\mathbb{R}^2)$ convergence $\nabla^{\mathfrak{D}_k}\mathbb{P}^{\overline{\mathcal{T}}_k}\varphi\to\nabla\varphi$. Using the weak-strong convergence in Lebesgue spaces, at the limit $k\to\infty$ we get

$$\int_\Omega\Upsilon\cdot\nabla\varphi\,\mathrm{d}x=\int_\Omega f\varphi\,\mathrm{d}x. \tag{4.5}$$

Identity (4.5) remains true for $\varphi \in W_0^{1,p}(\Omega)$, due to a standard density argument. Using the monotony of the operator $\boldsymbol{\alpha}$ and Minty's trick [33], following the guidelines of [8] or those of [19], we then establish that $\Upsilon = \boldsymbol{\alpha}(\cdot, \nabla u)$ a.e. in Ω. Proceeding again as in [8] or in [19], we establish that

$$\lim_{k\to+\infty} \int_\Omega \boldsymbol{\alpha}(x, \nabla^{\mathfrak{D}_k} u^{\overline{\mathcal{T}}_k}) \cdot \nabla^{\mathfrak{D}_k} u^{\overline{\mathcal{T}}_k} \,\mathrm{d}x = \int_\Omega \boldsymbol{\alpha}(x, \nabla u) \cdot \nabla u \,\mathrm{d}x,$$

and then, $\nabla^{\mathfrak{D}_k} u^{\overline{\mathcal{T}}_k} \to \nabla u$ a.e. on Ω and $\boldsymbol{\alpha}(\cdot, \nabla^{\mathfrak{D}_k} u^{\overline{\mathcal{T}}_k}) \cdot \nabla^{\mathfrak{D}_k} u^{\overline{\mathcal{T}}_k} \to \boldsymbol{\alpha}(\cdot, \nabla u) \cdot \nabla u$ in $L^1(\Omega)$. Now using the coercivity (1.2a) of $\boldsymbol{\alpha}$, by the Vitali theorem we prove that the weak convergence $\nabla^{\mathfrak{D}_k} u^{\overline{\mathcal{T}}_k} \to \nabla u$ is upgraded to the strong $L^p(\Omega; \mathbb{R}^2)$ convergence.

It remains to notice that, having proved that $u \in W_0^{1,p}(\Omega)$ and that $\Upsilon = \boldsymbol{\alpha}(\cdot, \nabla u)$, by the identity (4.5) we assert that u is the (unique) weak solution of problem (1.1). This concludes the proof. □

Remark 4.2. *(i) In the present paper, we investigate the order of convergence only numerically (see Section 6). However, let us stress that, if one assumes that the exact solution u belongs to $W^{2,p}(\Omega)$ and the space dependence of $\boldsymbol{\alpha}$ is smooth enough, then following the analysis of [8] one can address the issue of order of convergence of the NDD scheme. The expected provable convergence order is then of $h^{\frac{1}{p-1}}$ for $p \geq 2$ and of h^{p-1} if $1 < p \leq 2$. Note that for the isotropic p-laplacian, it is possible that sharper results can be obtained on highly symmetrical meshes in two complementary directions: the approximation of solutions with the typical fractional Sobolev regularity and superconvergence for very smooth solutions. We refer, respectively, to [6] and to [7], where such studies were asserted for a Finite Volume method on structured Cartesian meshes; this method is different from DDFV but the two methods share the same symmetries, on structured meshes. Finally, numerical tests of Section 6 demonstrate that the provable convergence orders are pessimistic in many cases, also with unstructured meshes. Proving superconvergence, e.g., in the standard DDFV context remains an open question.*

(ii) Further, in the case where $\boldsymbol{\alpha}$ involves jumps (typically, in case the diffusion matrix Λ in the example (1.3) is piecewise constant in x and the jumps occur along a subset of interfaces of the primal mesh), the convergence order expected in the smooth case is not achieved for the straightforward DDFV scheme. A solution to this problem, named m-DDFV, was proposed in [11]; it involves a precise and somewhat cumbersome modification of the DDFV gradient scheme in the diamonds that contain the jump; this is related to the necessity to average carefully the diffusion tensor over such a diamond.

In contrast to this situation, the NDD scheme need not be modified in the case where Λ in (1.3) possesses discontinuities across some of the primal interfaces. This is due to the fact that the NDD diamonds are half-diamonds of the DDFV mesh, and the diffusion tensor is constant in every NDD diamond whenever jumps in Λ occur across primal mesh interfaces. Therefore, the NDD scheme is self-sufficient in these situations where m-DDFV offers a substantial advantage over DDFV. This fact is illustrated in Test 5 of Section 6.

5 Adaptation(s) of the 2D NDD construction to the 3D case

Two 3D extensions of the 2D DDFV scheme were elaborated, called CeVe-DDFV and CeVeFE-DDFV (see [17, 29, 3, 2] and [16, 22], respectively). The CeVeFE-DDFV version exploits unknowns situated at the cell centers, cell vertices and also at edge centers, while the CeVe-DDFV version uses only the cell and the vertex unknowns. Recall that the key objective behind introducing the NDD scheme is to reduce the number of unknowns actually involved in the resolution of the algebraic system, while keeping the advantages of the DDFV approach. Thus, edge unknowns of the CeVeFE-DDFV method should be avoided. In this section, we propose two 3D extensions of the 2D NDD scheme - the two versions coincide in the case of meshes with triangular faces - based upon the cell unknowns (eliminated like in Section 3.4) and the vertex unknowns. The first one, called 3D fd-NDD, uses the same principle of gradient construction as the CeVe-DDFV method; it has the drawback of not being unconditionally coercive when the faces of the mesh are allowed to have an arbitrary number of vertices. The second one, called 3D sd-NDD, uses the same principle of gradient reconstruction as the CeVeFE-DDFV method, and enjoys unconditional coercivity; it has a more complex description and requires a finer diamond mesh than the 3D fd-NDD scheme. Here, the abbreviation

"3D fd-NDD" means *3D full-diamond Nodal Discrete Duality* while "3D sd-NDD" stands for *split-diamond Nodal Discrete Duality*, with the reference to the diamond partition. We will not sketch the convergence analysis for the 3D case, because it is quite analogous to the arguments of Section 4. We only outline the construction of the schemes, providing in each case the expression of the discrete gradient and divergence operators that ensure the Discrete Duality property, and highlighting the consistency properties of these operators.

5.1 The 3D fd-NDD construction

Given a polyhedral domain $\Omega \subset \mathbb{R}^3$, consider a mesh $\mathfrak{M}$ that consists of convex control volumes (cells). Let A denote a given volume, with $x_A \in A$ as its center. We denote by σ a generic face of the mesh $\mathfrak{M}$, while x_σ stands for the barycenter of the face σ. The set of all faces of the mesh is denoted by Σ; the set of faces that form the boundary of A is denoted by Σ_A. Given a face σ, we denote by ν_σ the set of its vertices, so that $\#\nu_\sigma$ is the number of vertices / of edges of $\sigma \in \Sigma$. We denote by e a generic edge of the mesh $\mathfrak{M}$; its center is denoted by x_e. The set of all edges of the mesh is denoted by $\mathcal{E}$. The set of the edges of a face $\sigma \in \Sigma_A$ form the subset $\mathcal{E}_\sigma$ of $\mathcal{E}$.

We denote a generic vertex of the mesh $\mathfrak{M}$ by $x_{A^\star}$. Further, we denote by $\Sigma_A^{A^\star}$ the set of all faces $\sigma \in \Sigma_A$ such that, in addition, $x_{A^\star}$ is a vertex of σ. Every vertex $x_{A^\star}$ of the primal mesh is considered as the center of a dual volume $A^\star$ that we define in the sequel. The set of all dual volumes is denoted by $\overline{\mathfrak{M}^\star}$. Given a face σ having $x_{A^\star}$ as one of its vertices, the set of all dual volumes which have for its center one of the vertices of σ is denoted by $\overline{\mathfrak{M}_\sigma^\star}$. Further, we denote by $\mathcal{E}_\sigma^{A^\star}$ the set of the two edges in $\mathcal{E}_\sigma$ having $x_{A^\star}$ as one of its vertices. Given $A \in \mathfrak{M}$, $\sigma \in \Sigma_A$ and $A^\star \in \overline{\mathfrak{M}^\star}$ such that $x_{A^\star}$ is a vertex of σ, we denote by $S_A^{A^\star}$ the convex envelope of x_A, x_σ, $x_{A^\star}$ and of $x_{e'}$, $x_{e''}$ where e', e'' are the two edges that constitute $\mathcal{E}_\sigma^{A^\star}$. Now, $A^\star$ is obtained as the union $\bigcup_{A:\, A^\star \in \overline{\mathfrak{M}_A^\star}} S_A^{A^\star}$.

The set of all dual volumes centered at the vertices $x_{A^\star}$ of the primal mesh such that $x_{A^\star} \in \Omega$ is denoted by $\mathfrak{M}^\star$ while the set of all boundary dual volumes (centered at $x_{A^\star} \in \partial\Omega$) is denoted by $\partial\mathfrak{M}^\star$, so that $\overline{\mathfrak{M}^\star}$ is the disjoint union $\mathfrak{M}^\star \cup \partial\mathfrak{M}^\star$. Finally, we define $\mathfrak{M}_{A^\star}$ as the subset of $\mathfrak{M}$ consisting of all primal volumes A such that $A^\star \in \overline{\mathfrak{M}_A^\star}$.

As in 2D, the diamonds of the 3D fd-NDD method (that are the half-diamonds of the 3D CeVe-DDFV method, cf. [3, 2]) are defined as the convex envelopes of x_A and σ for a primal volume $A \in \mathfrak{M}$ and its face $\sigma \in \Sigma_A$; the so obtained diamond is denoted $\mathcal{D}_{A,\sigma}$. The set of all diamonds of the 3D fd-NDD scheme is denoted by $\mathfrak{D}^{\mathrm{fd}}$ (note that the 3D sd-NDD construction in Section 5.2 uses a finer partitions into diamonds, that will be denoted $\mathfrak{D}^{\mathrm{sd}}$ in order to avoid confusion; the diamonds of the sd-NDD scheme will be labeled not only by $A \in \mathfrak{M}$ and $\sigma \in \Sigma_A$, but also by $e \in \mathcal{E}_\sigma$).

For $K \in \mathfrak{M} \cup \mathfrak{M}^\star$, $|K|$ stands for the volume (the three-dimensional Lebesgue measure) of the primal or dual volume K; similarly, $|\mathcal{D}|$ stands for the volume of a diamond $\mathcal{D} \in \mathfrak{D}^{\mathrm{fd}}$. For a face σ, $|\sigma|$ stands for its area (the two-dimensional Lebesgue measure). For an edge $e \in \mathcal{E}$, $|e|$ stands for its length.

Given a diamond $\mathcal{D}_{A,\sigma} \in \mathfrak{D}^{\mathrm{fd}}$, we define the primal normal $\mathbf{n}_{A,\sigma}$ as being the unit vector normal to σ pointing outside A. We will exploit the weighted primal normal vector ot the 3D fd-NDD method defined by

$$\mathbf{N}_{A,\sigma} = |\sigma|\mathbf{n}_{A,\sigma}$$

in the definition of both the discrete gradient and the discrete divergence operators. We will also need dual normals associated with a diamond $\mathcal{D}_{A,\sigma}$; their definition will involve a given vertex $x_{A^\star}$ of σ and an edge $e \in \mathcal{E}_\sigma^{A^\star}$. First, we denote by $\sigma^\star$ a generic part of the boundary of a generic dual volume $A^\star$ included in some diamond $\mathcal{D}_{A,\sigma}$; its area is denoted by $|\sigma^\star|$. Somewhat abusively, we say that $\sigma^\star$ is a dual face (in fact, it can be a portion of a plane face of the dual mesh). It is easily seen that each dual face $\sigma^\star$ can be associated in a unique way with $A \in \mathfrak{M}$, $\sigma \in \Sigma_A$ and $e \in \mathcal{E}_\sigma$; in this case, we denote it by $\sigma^\star_{A,\sigma,e}$. Given $x_{A^\star}$ an endpoint of e, we denote by $\mathbf{n}^{A^\star}_{A,\sigma,e}$ the unit vector normal to $\sigma^\star_{A,\sigma,e}$ pointing outside $A^\star$; and the corresponding weighted normal $\mathbf{N}^{A^\star}_{A,\sigma,e}$ is defined by

$$\mathbf{N}^{A^\star}_{A,\sigma,e} = |\sigma^\star_{A,\sigma,e}|\mathbf{n}^{A^\star}_{A,\sigma,e}.$$

As in 2D (cf. Remark 2.1), we will use a somewhat redundant notation for dual normals. Given an edge e, we denote its endpoints $x_{A^\star_e}$, $x_{B^\star_e}$ in an arbitrarily fixed order. Then, $\mathbf{n}^\star_{A,\sigma,e}$ will denote the unit normal vector

to $\sigma^\star_{A,\sigma,e}$ making an acute angle with the vector pointing from $x_{A^\star_e}$ to $x_{B^\star_e}$; and $\mathbf{N}^\star_{A,\sigma,e} = \left|\sigma^\star_{A,\sigma,e}\right| \mathbf{n}^\star_{A,\sigma,e}$ is the corresponding weighted normal. Observe that

$$\mathbf{N}^{A^\star}_{A,\sigma,e} = +\mathbf{N}^\star_{A,\sigma,e} \text{ if } A^\star = A^\star_e, \quad \text{and} \quad \mathbf{N}^{A^\star}_{A,\sigma,e} = -\mathbf{N}^\star_{A,\sigma,e} \text{ if } A^\star = B^\star_e. \tag{5.1}$$

Further, notations $\mathbb{R}^{\overline{\mathcal{T}}}_0$ and $(\mathbb{R}^3)^{\mathfrak{D}^{\rm fd}}$ for the spaces of discrete functions verifying the homogeneous Dirichlet boundary condition and for discrete vector-fields, respectively, keep the meaning analogous to the 2D case. In particular, given

$$v^{\mathcal{T}} = \Big((v_A)_{A\in\overline{\mathfrak{M}}}, (v_{A^\star})_{A^\star\in\overline{\mathfrak{M}^\star}} \Big),$$

we define by (2.3) the functions $v^{\mathfrak{M}}(\cdot)$, $v^{\overline{\mathfrak{M}^\star}}(\cdot)$ and then - differently from the 2D case - the function on Ω associated with the 3D NDD construction is defined by the weighted average

$$v^{\mathcal{T}}(x) = \frac{1}{3} v^{\mathfrak{M}}(x) + \frac{2}{3} v^{\overline{\mathfrak{M}^\star}}(x). \tag{5.2}$$

The 3D scalar product on the space of discrete functions is weighted the same way as (5.2): it is given by the bilinear form

$$\Big[\!\Big[v^{\mathcal{T}}, w^{\mathcal{T}} \Big]\!\Big]_{\mathcal{T}} = \frac{1}{3} \sum_{A\in\mathfrak{M}} |A|\, v_A w_A + \frac{2}{3} \sum_{A^\star\in\overline{\mathfrak{M}^\star}} |A^\star|\, v_{A^\star} w_{A^\star}. \tag{5.3}$$

At the same time, the inner product $\Big\{\!\!\Big\{ \cdot, \cdot \Big\}\!\!\Big\}$ on $(\mathbb{R}^3)^{\mathfrak{D}^{\rm fd}}$ (which is a scalar product, whenever the Poincaré inequality holds true, see Remark 5.1)) is defined in the same way as in 2D.

Let us now describe the per-diamond gradient reconstruction. Consider $A \in \mathfrak{M}$, $\sigma \in \mathcal{E}_A$ and $\mathcal{D} = \mathcal{D}_{A,\sigma}$. The degrees of freedom $v^{\mathcal{T}}$ of the 3D fd-NDD method involved in the construction of the discrete gradient are the value v_A associated with x_A and the $\#\nu_\sigma$ values $v_{A^\star}$ associated with the dual volumes $A^\star \in \Sigma_A$. In addition, the barycentric interpolated value

$$v_\sigma = \frac{1}{\#\nu_\sigma} \sum_{A^\star\in\overline{\mathfrak{M}^\star_A}} v_{A^\star}, \tag{5.4}$$

plays a role in the definition of the discrete gradient.

The 3D fd-NDD scheme uses the discrete gradient obtained as in [3] (which coincides with the constructions in [29, 17] under appropriate notational changes). Given $v^{\mathcal{T}}$, to define $\nabla_{\mathcal{D}_{A,\sigma}} v^{\overline{\mathcal{T}}}$ we take the vector which projection on the direction $x_A x_\sigma$ is obtained using the finite difference $v_\sigma - v_A$; while its projection on the plane containing the face σ is reconstructed as a combination of the $\#\nu_\sigma$ finite differences $v_{B^\star_e} - v_{A^\star_e}$, $e \in \mathcal{E}_\sigma$, according to the formula put forward in [4, 7] which reads as follows, with the above notation:

$$\nabla_{\mathcal{D}_{A,\sigma}} v^{\overline{\mathcal{T}}} = \frac{1}{3\,|\mathcal{D}_{A,\sigma}|} \Big((v_\sigma - v_A)\, \mathbf{N}_{A,\sigma} \,+\, 2 \sum_{e\in\mathcal{E}_\sigma} (v_{B^\star_e} - v_{A^\star_e}) \mathbf{N}^\star_{A,\sigma,e} \Big), \quad \text{for } \mathcal{D} = \mathcal{D}_{A,\sigma} \in \mathfrak{D}^{\rm fd}. \tag{5.5}$$

We stress the fact that, irrespective of the value of $\#\nu_\sigma$, this approximation is exact on affine functions, i.e., in the case u_A, $u_{A^\star}$ for $A^\star \in \overline{\mathfrak{M}^\star_A}$ are the values, at the corresponding points x_A, $x_{A^\star}$, of an affine function $\varphi : \mathcal{D}_{A,\sigma} \to \mathbb{R}$, one has $\nabla_{\mathcal{D}_{A,\sigma}} v^{\overline{\mathcal{T}}} = \nabla\varphi$ (see [3, App. A]). In particular, whenever $\#\nu_\sigma = 3$, the resulting discrete gradient reconstruction is the standard $\mathbb{P}_1$ gradient reconstruction in the tetrahedron $\mathcal{D}_{A,\sigma}$. Further, the exactness property implies that the consistency claim analogous to the 2D claim of Proposition 2.1 holds true.

Remark 5.1. *Let us point out that the validity of the Poincaré inequality is an issue, for the 3D fd-NDD construction (exactly as for the 3D CeVe-DDFV construction). The equivalence with the $\mathbb{P}_1$ reconstruction ensures that the Poincaré inequality holds true if all faces of the primal mesh $\mathfrak{M}$ are triangles. It is proved in [2] that 3D CeVe-DDFV on Cartesian meshes still possesses this property, and it is expected that under appropriate regularity assumptions, the Poincaré inequality remain valid for meshes which faces are either triangles or quadrangles. However, if $\#\nu_\sigma$ can take large values, the 3D fd-NDD scheme may lack coercivity. This is the reason why the 3D sd-NDD scheme described below is preferable to 3D fd-NDD, at least from the viewpoint of the theoretical convergence analysis. The practical comparison of the two 3D NDD schemes will be carried out in the forthcoming contribution [9].*

We now define the discrete divergence operator of the 3D fd-NDD method. Given a discrete vector-field $\mathcal{F}^{\mathfrak{D}}$ (for the sake of legibility we write $\mathcal{F}^{\mathfrak{D}}$, meaning $\mathfrak{D} = \mathfrak{D}^{\mathrm{fd}}$ for the sd-NDD method), the primal components of $\mathrm{div}^{\mathcal{T}}\, \mathcal{F}^{\mathfrak{D}}$ are defined by

$$\mathrm{div}_A\ \mathcal{F}^{\mathfrak{D}} := \frac{1}{|A|} \sum_{\sigma \in \Sigma_A} \mathcal{F}_{\mathcal{D}_{A,\sigma}} \cdot \mathbf{N}_{A,\sigma}, \quad \forall A \in \mathfrak{M}.$$

As for the 2D NDD scheme, in the dual cell the definition of the discrete divergence is not a straightforward analogue of the previous one. Our aim in introducing a non-obvious definition is to properly account for the discrete duality relationship (see Proposition 5.1). We set

$$\mathrm{div}_{A^\star}\ \mathcal{F}^{\mathfrak{D}} := \frac{1}{|A^\star|} \sum_{A \in \mathfrak{M}_{A^\star}} \sum_{\sigma \in \Sigma_A^{A^\star}} \sum_{e \in \mathcal{E}_\sigma^{A^\star}} \mathcal{F}_{\mathcal{D}_{A,\sigma}} \cdot \widetilde{\mathbf{N}_{A,\sigma,e}^{A^\star}}, \quad \forall A^\star \in \mathfrak{M}^\star,$$

where the *modified dual normal* $\widetilde{\mathbf{N}_{A,\sigma,e}^{A^\star}}$ is given by the formula

$$\widetilde{\mathbf{N}_{A,\sigma,e}^{A^\star}} := \mathbf{N}_{A,\sigma,e}^{A^\star} - \frac{1}{4\#\nu_\sigma} \mathbf{N}_{A,\sigma}. \tag{5.6}$$

We now provide the Discrete Duality property linking the 3D fd-NDD discrete operators.

Proposition 5.1. *The 3D fd-NDD discrete gradient and discrete divergence operators enjoy the discrete duality property*

$$\forall \varphi^{\mathcal{T}} \in \mathbb{R}_0^{\mathcal{T}}\ \ \forall \mathcal{F}^{\mathfrak{D}} \in (\mathbb{R}^3)^{\mathfrak{D}^{\mathrm{fd}}} \qquad \Big[\!\Big[\mathrm{div}^{\mathcal{T}}\, \mathcal{F}^{\mathfrak{D}}\, ,\, \varphi^{\mathcal{T}} \Big]\!\Big]_{\mathcal{T}} = -\Big\{\!\Big\{ \mathcal{F}^{\mathfrak{D}}\, ,\, \nabla^{\mathfrak{D}} \varphi^{\overline{\mathcal{T}}} \Big\}\!\Big\}_{\mathfrak{D}}, \tag{5.7}$$

having in mind the definition (5.3) *of* $\Big[\!\Big[\cdot,\cdot\Big]\!\Big]_{\mathcal{T}}$ *proper to the 3D case.*

Proof. We follow closely the proof of Proposition 2.2. Using the definition (5.3) of $\Big[\!\Big[\cdot,\cdot\Big]\!\Big]_{\mathcal{T}}$, we split left hand side of (5.7) to obtain

$$\Big[\!\Big[\mathrm{div}^{\mathcal{T}}\, \mathcal{F}^{\mathfrak{D}}\, ,\, \varphi^{\mathcal{T}} \Big]\!\Big]_{\mathcal{T}} = \frac{1}{3}(X + Y + Z),$$

where we separated the contribution X of $\mathfrak{M}$, and splitted the contribution of $\mathfrak{M}^\star$ into terms Y and Z according to the right-hand side of (5.6):

$$X = \sum_{A \in \mathfrak{M}} \sum_{\sigma \in \Sigma_A} \varphi_A\, \mathcal{F}_{\mathcal{D}_{A,\sigma}} \cdot \mathbf{N}_{A,\sigma}, \quad Y = 2 \sum_{A^\star \in \mathfrak{M}^\star} \sum_{A \in \mathfrak{M}_{A^\star}} \sum_{\sigma \in \Sigma_A^{A^\star}} \sum_{e \in \mathcal{E}_\sigma^{A^\star}} \varphi_{A^\star}\, \mathcal{F}_{\mathcal{D}_{A,\sigma}} \cdot \mathbf{N}_{A,\sigma,e}^{A^\star},$$
$$Z = -\frac{2}{4\#\nu_\sigma} \sum_{A^\star \in \mathfrak{M}^\star} \sum_{A \in \mathfrak{M}_{A^\star}} \sum_{\sigma \in \Sigma_A^{A^\star}} \sum_{e \in \mathcal{E}_\sigma^{A^\star}} \varphi_{A^\star}\, \mathcal{F}_{\mathcal{D}_{A,\sigma}} \cdot \mathbf{N}_{A,\sigma}.$$

Bear in mind that for $A_e^\star, B_e^\star$ such that $e = [x_{A_e^\star}, x_{B_e^\star}]$, in the expression Y we find the same vector $\mathcal{F}_{\mathcal{D}_{A,\sigma}}$ multiplied by the two opposite normal vectors (see (5.1) to yield

$$\mathcal{F}_{\mathcal{D}_{A,\sigma}} \cdot \mathbf{N}_{A,\sigma,e}^{B_e^\star} = -\mathcal{F}_{\mathcal{D}_{A,\sigma}} \cdot \mathbf{N}_{A,\sigma,e}^{A_e^\star}, \tag{5.8}$$

which expresses the conservativity of the fluxes appearing in the sum Y. This permits to rearrange the summation of Y per diamond. We arrive to

$$Y = 2 \sum_{A \in \mathfrak{M}} \sum_{\sigma \in \Sigma_A} \sum_{e \in \mathcal{E}_\sigma} (\varphi_{A_e^\star} - \varphi_{B_e^\star})\, \mathcal{F}_{\mathcal{D}_{A,\sigma}} \cdot \mathbf{N}_{A,\sigma,e}^\star.$$

Then, we rearrange per diamond the expression in Z before combining it with X; recall that the fd-NDD diamonds are labeled by $A \in \mathfrak{M}$, $\sigma \in \Sigma_A$. This rearrangement makes appear the inner sum $\sum_{A^\star \in \overline{\mathfrak{M}_\sigma^\star}} \sum_{e \in \mathcal{E}_\sigma^{A^\star}}$

featuring the same flux $\mathcal{F}_{\mathcal{D}_{A,\sigma}} \cdot \mathbf{N}_{A,\sigma}$, where each of the factors $\varphi_{A^\star}$, $A^\star \in \overline{\mathfrak{M}^\star_\sigma}$, appears twice because each edge has two extremities. Accordingly, the expression of Z can be reordered as follows:

$$Z = -\sum_{A\in\mathfrak{M}} \sum_{\sigma\in\Sigma_A} \varphi_\sigma \, \mathcal{F}_{\mathcal{D}_{A,\sigma}} \cdot \mathbf{N}_{A,\sigma}, \quad \text{where we recall that } \varphi_\sigma = \frac{1}{\#\nu_\sigma} \sum_{A^\star\in\overline{\mathfrak{M}^\star_\sigma}} \varphi_{A^\star}.$$

The expression of X is already written per diamond. This allows its combination to the terms of Z. Thereby, we infer

$$\frac{1}{3}(X+Y+Z) = \sum_{A\in\mathfrak{M}} \sum_{\sigma\in\Sigma_A} \mathcal{F}_{\mathcal{D}_{A,\sigma}} \cdot \frac{1}{3}\bigg((\varphi_A - \varphi_\sigma)\mathbf{N}_{A,\sigma} \, + \, 2 \sum_{e\in\mathcal{E}_\sigma} (\varphi_{A^\star_e} - \varphi_{B^\star_e})\mathbf{N}^\star_{A,\sigma,e} \bigg).$$

To conclude, the result is obtained by dividing and multiplying by $|D_{A,\sigma}|$ each term of the sum, because we find the expression (2.7) (with the minus sign) in the last factor of the above equation. This conducts us to the sought identification of $\Big[\!\Big[\operatorname{div}^{\mathcal{T}} \mathcal{F}^{\mathfrak{D}} \, , \, \varphi^{\mathcal{T}} \Big]\!\Big]_{\mathcal{T}} = \frac{1}{3}(X+Y+Z)$ with $\Big\{\!\!\Big\{ \mathcal{F}^{\mathfrak{D}} \, , \, -\nabla^{\mathfrak{D}} \varphi^{\overline{\mathcal{T}}} \Big\}\!\!\Big\}_{\mathfrak{D}}$. □

Calculations analogous to the Discrete Duality feature also permit to ascertain the weak (dual) consistency of the NDD discrete divergence operator. Indeed, the suitable projection $\mathbb{P}^{\mathfrak{D}}$ of a smooth vector-field ψ on the diamond mesh $\mathfrak{D}^{\mathrm{fd}}$ is defined, as in 2D, by taking the average face value $\psi_\sigma := \frac{1}{|\sigma|}\int_\sigma \psi$ as the common value $\psi_{\mathcal{D}_{A,\sigma}}$ and $\psi_{\mathcal{D}_{B,\sigma}}$ in the diamonds $\mathcal{D}_{A,\sigma}, \mathcal{D}_{B,\sigma}$. Here we mean that the face $\sigma = A|B$ separates two primal volumes denoted by A and B. We infer the 3D analogue of the weak consistency claim of Proposition 2.3 for the discrete divergence operator, adapting in a straightforward way the 2D proof.

To sum up, we presented the 3D fd-NDD construction, justified the Discrete Duality property and the adequate consistency properties of the discrete gradient and the discrete divergence operators. Now the 3D fd-NDD discretization of problem (1.1) can be done exactly as in the 2D case. Under the additional coercivity assumptions discussed in Remark 5.1 and the mesh regularity assumptions typical of the 3D DDFV schemes (cf. [2, 16]), the convergence analysis of Section 4 remains relevant.

Moreover, as in 2D, the resulting scheme presents the following advantages over the 3D CeVe-DDFV scheme:

- it permits an easy algebraic elimination of the cell unknowns;
- it does not require the use of a penalization operator for assessing convergence;
- it does not require any specific adaptation to the case of piecewise continuous diffusion tensors, if the discontinuities occur across faces of the primal mesh.

The possible lack of coercivity, when faces with many vertices are present in the mesh, is the drawback shared by the 3D CeVe-DDFV and the 3D fd-NDD schemes.

5.2 The 3D sd-NDD construction

In this section, we present the more intricate 3D sd-NDD ("split-diamond") method, which has the advantage of unconditional coercivity over the 3D fd-NDD ("full-diamond") method. The construction of the primal and the dual meshes and the associated notation remain unchanged. The sd-NDD diamond partition, denoted $\mathfrak{D}^{\mathrm{sd}}$, is finer than the fd-NDD partition $\mathfrak{D}^{\mathrm{fd}}$. More precisely, a diamond of the sd-NDD mesh is labeled by a primal volume $A \in \mathfrak{M}$, a face $\sigma \in \Sigma_A$ of this primal volume, and also by an edge $e \in \mathcal{E}_\sigma$ of this face; recall that the fd-NDD diamonds are labeled only by A and σ. Each fd-diamond $\mathcal{D}_{A,\sigma} \in \mathfrak{D}^{\mathrm{fd}}$ is split into the union of $\#\nu_\sigma$ sd-diamonds $\mathcal{D}_{A,\sigma,e} \in \mathfrak{D}^{\mathrm{sd}}$; $\mathcal{D}_{A,\sigma,e}$ is the tetrahedron with vertices x_A, x_σ, $x_{A^\star_e}$, $x_{B^\star_e}$.

The dual normals $\mathbf{N}^\star_{A,\sigma,e}$, $\mathbf{N}^{A^\star}_{A,\sigma,e}$ (with the convention (5.1)) are defined exactly as for the 3D fd-NDD method. To define the primal normal per sd-diamond, for $\sigma \in \Sigma$ and $e \in \mathcal{E}_\sigma$ we write σ_e for the triangle in the face σ with vertices x_σ, $x_{A^\star_e}$, $x_{B^\star_e}$; as usual, $|\sigma_e|$ stands for the area (the two-dimensional Lebesgue measure) of σ_e. We will exploit the weighted primal normal vector of the 3D sd-NDD method defined by

$$\mathbf{N}_{A,\sigma,e} = |\sigma_e| \mathbf{n}_{A,\sigma},$$

in the definition of both the discrete gradient and the discrete divergence operators. Note in passing that

$$\mathbf{N}_{A,\sigma} = \sum_{e \in \mathcal{E}_\sigma} \mathbf{N}_{A,\sigma,e}, \tag{5.9}$$

where $\mathbf{N}_{A,\sigma}$ is the weighted normal involved in the fd-NDD method. Further, inspired by the 3D CeVeFE-DDFV construction, we define the third family of weighted normal vectors associated with sd-diamonds. Given $e \in \mathcal{E}$, we denote $x_e = \frac{1}{2}(x_{A_e^\star} + x_{B_e^\star})$ its center. We set[5]

$$\mathbf{N}^{\#}_{A,\sigma,e} = (-1)^{\epsilon_e} \frac{1}{2} \overrightarrow{x_A x_\sigma} \wedge \overrightarrow{x_{A_e^\star} x_{B_e^\star}} \tag{5.10}$$

with the choice $\epsilon_e \in \{0,1\}$ made in order that $\mathbf{N}^{\#}_{A,\sigma,e}$ form an acute angle with the vector pointing from x_σ to x_e. E.g. in the case where $\overrightarrow{x_A x_\sigma}$ is orthogonal to σ, the vector $\mathbf{N}^{\#}_{A,\sigma,e}$ stands for the appropriately weighted vector lying in the plane σ, normal to e and pointing outside σ.

The 3D sd-NDD discrete gradient operator is defined per sd-diamond $\mathcal{D} = \mathcal{D}_{A,\sigma,e}$ as follows. Given a discrete function $v^{\mathcal{T}}$, in addition to the values v_A, $v_{A_e^\star}$, $v_{B_e^\star}$ and the value v_σ defined in (5.4) we also introduce

$$v_e = \frac{1}{2}(v_{A_e^\star} + v_{B_e^\star}). \tag{5.11}$$

Then, the value of $\nabla^{\mathfrak{D}} v^{\overline{\mathcal{T}}}$ in the diamond $\mathcal{D}_{A,\sigma,e}$ is defined by the formula

$$\nabla_{\mathcal{D}_{A,\sigma,e}} v^{\overline{\mathcal{T}}} = \frac{1}{3\,|\mathcal{D}_{A,\sigma,e}|} \left((v_\sigma - v_A)\,\mathbf{N}_{A,\sigma,e} + (v_{B^\star} - v_{A^\star})\,\mathbf{N}^{A^\star}_{A,\sigma,e} + (v_e - v_\sigma)\,\mathbf{N}^{\#}_{A,\sigma,e} \right). \tag{5.12}$$

This definition is the same as the 3D CeVeFE-DDFV discrete gradient, being understood that in the CeVeFE-DDFV setting the values v_σ and v_e are additional unknowns while our sd-NDD method uses the interpolated values (5.4) and (5.11), respectively. Because both the interpolation formulas (5.4), (5.11) and the CeVeFE-DDFV discrete gradient formula are exact on affine functions on the diamond $\mathcal{D}_{A,\sigma,e}$ (see, in particular, [16]), the formula (5.12) is exact on affine functions. As in the 2D and in the 3D fd-NDD setting, this readily implies the consistency of the 3D sd-NDD discrete gradient operator in the sense analogous to Proposition 2.1.

Remark 5.2. *Observe that, in the case $\#\nu_\sigma = 3$, the sd-NDD gradient reconstruction coincides with the $\mathbb{P}_1$ reconstruction and with the fd-NDD reconstruction.*

Let us now define the 3D sd-NDD discrete divergence operator acting from $(\mathbb{R}^3)^{\mathfrak{D}^{\mathrm{sd}}}$ to $\mathbb{R}^{\mathcal{T}}$. Given a discrete vector-field $\mathcal{F}^{\mathfrak{D}} \in (\mathbb{R}^3)^{\mathfrak{D}^{\mathrm{sd}}}$, the value of $\mathrm{div}^{\mathcal{T}}\,\mathcal{F}^{\mathfrak{D}}$ in a primal cell A is simply given by

$$\mathrm{div}_A\,\mathcal{F}^{\mathfrak{D}} = \frac{1}{|A|} \sum_{\sigma \in \Sigma_A} \sum_{e \in \mathcal{E}_\sigma} \mathcal{F}_{\mathcal{D}_{A,\sigma,e}} \cdot \mathbf{N}_{A,\sigma,e}, \quad \forall A \in \mathfrak{M}.$$

In a dual cell $A^\star$, the definition of the discrete divergence is an involved one, it can be inferred from the desired discrete duality relationship (see Proposition 5.2). We set

$$\mathrm{div}_{A^\star}\,\mathcal{F}^{\mathfrak{D}} := \frac{1}{|A^\star|} \sum_{A \in \mathfrak{M}_{A^\star}} \sum_{\sigma \in \Sigma_A^{A^\star}} \left\{ \sum_{e \in \mathcal{E}_\sigma^{A^\star}} \mathcal{F}_{\mathcal{D}_{A,\sigma,e}} \cdot \widetilde{\mathbf{N}^{A^\star}_{A,\sigma,e}} + \sum_{e \in \mathcal{E}_\sigma} \mathcal{F}_{\mathcal{D}_{A,\sigma,e}} \cdot \widehat{\mathbf{N}_{A,\sigma,e}} \right\}, \quad \forall A^\star \in \mathfrak{M}^\star,$$

where the *modified dual normal* $\widetilde{\mathbf{N}^{A^\star}_{A,\sigma,e}}$ (appearing within the summation over the two edges that constitute $\mathcal{E}_\sigma^{A^\star}$) is given by the formula

$$\widetilde{\mathbf{N}^{A^\star}_{A,\sigma,e}} := \frac{1}{2}\mathbf{N}^{A^\star}_{A,\sigma,e} - \frac{1}{4}\mathbf{N}^{\#}_{A,\sigma,e} \tag{5.13}$$

[5]Exceptionally, we use the arrow notation $\overrightarrow{\cdot}$ for vectors defined by their endpoints it the context of (5.10) and in the proof of Lemma 5.1 below; but we omit $\overrightarrow{\cdot}$ from the notation of all the weighted normals like $\mathbf{N}_{A,\sigma}$, $\mathbf{N}^{\#}_{A,\sigma,e}$ and from those of discrete and continuous vector-fields like gradients and fluxes.

and in addition, in the summation featuring $\#\nu_\sigma$ edges constituting $\mathcal{E}_\sigma$, there appears

$$\widehat{\mathbf{N}_{A,\sigma,e}} := \frac{1}{2\#\nu_\sigma}\Big(-\mathbf{N}_{A,\sigma,e} + \mathbf{N}^{\#}_{A,\sigma,e}\Big). \tag{5.14}$$

We now provide the Discrete Duality property linking the 3D sd-NDD discrete operators; note that the definitions of the inner products on the spaces of discrete functions and of discrete fields keep the same form as for the fd-NDD method.

Proposition 5.2. *The 3D sd-NDD discrete gradient and discrete divergence operators enjoy the discrete duality property*

$$\forall \varphi^{\mathcal{T}} \in \mathbb{R}_0^{\overline{\mathcal{T}}} \;\; \forall \mathcal{F}^{\mathfrak{D}} \in (\mathbb{R}^3)^{\mathfrak{D}^{\rm sd}} \qquad \Big[\!\Big[\operatorname{div}^{\mathcal{T}} \mathcal{F}^{\mathfrak{D}} \, , \, \varphi^{\mathcal{T}} \Big]\!\Big]_{\mathcal{T}} = -\Big\{\!\!\Big\{ \mathcal{F}^{\mathfrak{D}} \, , \, \nabla^{\mathfrak{D}} \varphi^{\overline{\mathcal{T}}} \Big\}\!\!\Big\}_{\mathfrak{D}}, \tag{5.15}$$

having in mind the definition (5.3) *of* $\Big[\!\Big[\cdot,\cdot\Big]\!\Big]_{\mathcal{T}}$ *proper to the 3D case.*

Proof. The definition (5.3) of the 3D bracket $\Big[\!\Big[\cdot,\cdot\Big]\!\Big]_{\mathcal{T}}$ allows the decomposition of the left hand side of (5.15) as follows:

$$\Big[\!\Big[\operatorname{div}^{\mathcal{T}} \mathcal{F}^{\mathfrak{D}}, \varphi^{\mathcal{T}} \Big]\!\Big]_{\mathcal{T}} = \frac{1}{3}(X + Y + U + Z + V),$$

where

$$\begin{aligned}
X &= \sum_{A\in\mathfrak{M}} \sum_{\sigma\in\Sigma_A} \sum_{e\in\mathcal{E}_\sigma} \varphi_A \mathcal{F}_{\mathcal{D}_{A,\sigma,e}} \cdot \mathbf{N}_{A,\sigma,e},\\
Y &= \sum_{A^\star\in\mathfrak{M}^\star} \sum_{A\in\mathfrak{M}_{A^\star}} \sum_{\sigma\in\Sigma_A^{A^\star}} \sum_{e\in\mathcal{E}_\sigma^{A^\star}} \varphi_{A^\star} \mathcal{F}_{\mathcal{D}_{A,\sigma,e}} \cdot \mathbf{N}^{A^\star}_{A,\sigma,e}\\
U &= -\frac{1}{2} \sum_{A^\star\in\mathfrak{M}^\star} \sum_{A\in\mathfrak{M}_{A^\star}} \sum_{\sigma\in\Sigma_A^{A^\star}} \sum_{e\in\mathcal{E}_\sigma^{A^\star}} \varphi_{A^\star} \mathcal{F}_{\mathcal{D}_{A,\sigma,e}} \cdot \mathbf{N}^{\#}_{A,\sigma,e},\\
Z &= -\frac{1}{\#\nu_\sigma} \sum_{A^\star\in\mathfrak{M}^\star} \sum_{A\in\mathfrak{M}_{A^\star}} \sum_{\sigma\in\Sigma_A^{A^\star}} \sum_{e\in\mathcal{E}_\sigma} \varphi_{A^\star} \mathcal{F}_{\mathcal{D}_{A,\sigma,e}} \cdot \mathbf{N}_{A,\sigma,e},\\
V &= \frac{1}{\#\nu_\sigma} \sum_{A^\star\in\mathfrak{M}^\star} \sum_{A\in\mathfrak{M}_{A^\star}} \sum_{\sigma\in\Sigma_A^{A^\star}} \sum_{e\in\mathcal{E}_\sigma} \varphi_{A^\star} \mathcal{F}_{\mathcal{D}_{A,\sigma,e}} \cdot \mathbf{N}^{\#}_{A,\sigma,e}.
\end{aligned}$$

Recall that for each each edge $e = [x_{A^\star_e}, x_{B^\star_e}]$, there holds

$$\mathcal{F}_{\mathcal{D}_{A,\sigma,e}} \cdot N^{A^\star}_{A,\sigma,e} = -\mathcal{F}_{\mathcal{D}_{A,\sigma,e}} \cdot N^{B^\star}_{A,\sigma,e}.$$

Rearranging the summation of Y per diamond, using the convention (5.1) we find

$$Y = \sum_{A\in\mathfrak{M}} \sum_{\sigma\in\Sigma_A^{A^\star}} \sum_{e\in\mathcal{E}_\sigma} (\varphi_{A^\star_e} - \varphi_{B^\star_e}) \mathcal{F}_{\mathcal{D}_{A,\sigma,e}} \cdot \mathbf{N}^{A^\star}_{A,\sigma,e}.$$

Then, we transform the expression of Z before combining it with X, gathering terms per diamond; recall that the sd-NDD diamonds are labeled by $A \in \mathfrak{M}$, $\sigma \in \Sigma_A$ and $e \in \mathcal{E}_\sigma$. This rearrangement makes appear the inner sum $\sum_{A^\star\in\overline{\mathfrak{M}^\star_\sigma}}$ featuring the same flux $\mathcal{F}_{\mathcal{D}_{A,\sigma}} \cdot \mathbf{N}_{A,\sigma,e}$, where each of the factors $\varphi_{A^\star}$, $A^\star \in \overline{\mathfrak{M}^\star_\sigma}$, appears exactly one time. We find

$$X + Z = \sum_{A\in\mathfrak{M}} \sum_{\sigma\in\Sigma_A} \sum_{e\in\mathcal{E}_\sigma} (\varphi_A - \varphi_\sigma) \mathcal{F}_{\mathcal{D}_{A,\sigma,e}} \cdot \mathbf{N}_{A,\sigma,e}, \quad \text{bearing in mind that } \varphi_\sigma = \frac{1}{\#\nu_\sigma} \sum_{A^\star\in\overline{\mathfrak{M}^\star_\sigma}} \varphi_{A^\star}.$$

Next, we reorder the summation in the terms U and V per diamond, before combining the two terms. We handle V in the same way as Z. As to the term U, gathering terms per diamond makes appear the inner

sum $\sum_{A^\star:\, e\in\mathcal{E}_\sigma^{A^\star}}$ so that the same flux $\mathcal{F}_{\mathcal{D}_{A,\sigma,e}}\cdot\mathbf{N}^{\#}_{A,\sigma,e}$ appears twice, weighted by $\varphi_{A^\star_e}$ and $\varphi_{B^\star_e}$, respectively. We infer

$$U+V=\sum_{A\in\mathfrak{M}}\sum_{\sigma\in\Sigma_A}\sum_{e\in\mathcal{E}_\sigma}(\varphi_\sigma-\varphi_e)\,\mathcal{F}_{\mathcal{D}_{A,\sigma,e}}\cdot\mathbf{N}^{\#}_{A,\sigma,e},\quad\text{bearing in mind that }\varphi_e=\frac{1}{2}\big(\varphi_{A^\star_e}+\varphi_{B^\star_e}\big).$$

As a consequence, one finds for the sum $\frac{1}{3}\big(X+Y+U+Z+V\big)=\Big[\!\Big[\operatorname{div}^{\mathcal{T}}\mathcal{F}^{\mathfrak{D}},\varphi^{\mathcal{T}}\Big]\!\Big]_{\mathcal{T}}$ the expression

$$\sum_{A\in\mathfrak{M}}\sum_{\sigma\in\Sigma_A}\sum_{e\in\mathcal{E}_\sigma}\mathcal{F}_{\mathcal{D}_{A,\sigma,e}}\cdot\frac{1}{3}\bigg((\varphi_A-\varphi_\sigma)\,\mathbf{N}_{A,\sigma,e}+(\varphi_{A^\star_e}-\varphi_{B^\star_e})\mathbf{N}^{\star}_{A,\sigma,e}+(\varphi_\sigma-\varphi_e)\,\mathbf{N}^{\#}_{A,\sigma,e}\bigg).$$

The required identity is obtained by multiplying and dividing each term of the sum by $-|\mathcal{D}_{A,\sigma,e}|$, having in mind the definition (5.12) of $\nabla_{\mathcal{D}_{A,\sigma,e}}\varphi^{\mathcal{T}}$. This concludes the proof. □

The consistency of the sd-NDD discrete divergence operator, in the sense analogous to (2.13) relies upon the following elementary geometrical observations.

Lemma 5.1. *Let $A\in\mathfrak{M}$, $\sigma\in\Sigma_A$. Keeping in mind the orientation convention for the vectors $\mathbf{N}^{\#}_{A,\sigma,e}$ defined in* (5.10)*, with the definition* (5.13) *of $\widetilde{\mathbf{N}^{A^\star}_{A,\sigma,e}}$ there holds*

$$\sum_{e\in\mathcal{E}_\sigma}\mathbf{N}^{\#}_{A,\sigma,e}=0,\tag{5.16}$$

$$\sum_{e\in\mathcal{E}_\sigma^{A^\star}}\widetilde{\mathbf{N}^{A^\star}_{A,\sigma,e}}=\sum_{e\in\mathcal{E}_\sigma^{A^\star}}\mathbf{N}^{A^\star}_{A,\sigma,e}.\tag{5.17}$$

Proof. We fix $A\in\mathfrak{M}$ and $\sigma\in\Sigma_A$. Then, we label the vertices of σ sequentially (clockwise, if one looks at σ from x_A) by $x_{A^\star_1},\,\dots,\,x_{A^\star_{\#\nu_\sigma}}\equiv x_{A^\star_0}$ and we denote by $e_{i+1/2}$, where $i=0,\dots,(\#\nu_\sigma-1)$, the edge $[x_{A^\star_i},x_{A^\star_{i+1}}]$, in such a way that

$$\mathbf{N}^{\#}_{A,\sigma,e_{i+1/2}}=+\frac{1}{2}\overrightarrow{x_Ax_\sigma}\wedge\overrightarrow{x_{A^\star_i}x_{A^\star_{i+1}}}.$$

Then we assert (5.16) by observing that

$$\sum_{e\in\mathcal{E}_\sigma}\mathbf{N}^{\#}_{A,\sigma,e}=\sum_{i=0}^{\#\nu_\sigma-1}\mathbf{N}^{\#}_{A,\sigma,e_{i+1/2}}=\frac{1}{2}\overrightarrow{x_Ax_\sigma}\wedge\sum_{i=0}^{\#\nu_\sigma-1}\overrightarrow{x_{A^\star_i}x_{A^\star_{i+1}}}=\frac{1}{2}\overrightarrow{x_Ax_\sigma}\wedge 0=0.\tag{5.18}$$

Further, notice that due to (5.13), proving (5.17) boils down to proving

$$-\frac{1}{2}\sum_{e\in\mathcal{E}_\sigma^{A^\star}}\mathbf{N}^{\#}_{A,\sigma,e}=\sum_{e\in\mathcal{E}_\sigma^{A^\star}}\mathbf{N}^{A^\star}_{A,\sigma,e}.\tag{5.19}$$

Keeping the numbering convention introduced for the sake of proving (5.16), we can further assume that $A^\star=A^\star_1$, so that $\mathcal{E}_\sigma^{A^\star}$ consists of $e_{1/2}=[x_{A^\star_0},x_{A^\star}]$ and $e_{3/2}=[x_{A^\star},x_{A^\star_2}]$; we denote by $x_{e_{1/2}}$, $x_{e_{3/2}}$ the midpoints of the respective edges. Observe that in a way analogous to (5.18), we can write the vectors $\mathbf{N}^{A^\star}_{A,\sigma,e_{1/2}}$, $\mathbf{N}^{A^\star}_{A,\sigma,e_{3/2}}$ normal to $\partial A^\star$ pointing outside $A^\star$ and weighted by the areas of the triangles $x_Ax_\sigma x_{e_{1/2}}$, $x_Ax_\sigma x_{e_{3/2}}$, respectively, as

$$\mathbf{N}^{A^\star}_{A,\sigma,e_{1/2}}=+\frac{1}{2}\overrightarrow{x_Ax_\sigma}\wedge\overrightarrow{x_\sigma x_{e_{1/2}}},\qquad\mathbf{N}^{A^\star}_{A,\sigma,e_{3/2}}=-\frac{1}{2}\overrightarrow{x_Ax_\sigma}\wedge\overrightarrow{x_\sigma x_{e_{3/2}}},$$

so that, using the Thales theorem and the definition of $e_{1/2}$ and $e_{3/2}$, we find

$$\sum_{e\in\mathcal{E}_\sigma^{A^\star}}\mathbf{N}^{A^\star}_{A,\sigma,e}=\frac{1}{2}\overrightarrow{x_Ax_\sigma}\wedge\overrightarrow{x_{e_{3/2}}x_{e_{1/2}}}=\frac{1}{4}\overrightarrow{x_Ax_\sigma}\wedge\overrightarrow{x_{A^\star_2}x_{A^\star_0}}.$$

The result (5.19) follows from considering the triangle with vertices $A_0^\star$, $A^\star = A_1^\star$, $A_2^\star$:

$$\frac{1}{2}\sum_{e\in\mathcal{E}_\sigma^{A^\star}} \mathbf{N}_{A,\sigma,e}^{\#} + \sum_{e\in\mathcal{E}_\sigma^{A^\star}} \mathbf{N}_{A,\sigma,e}^{A^\star} = \frac{1}{4}\overrightarrow{x_A x_\sigma} \wedge \Big(\overrightarrow{x_{A_0^\star} x_{A_1^\star}} + \overrightarrow{x_{A_1^\star} x_{A_2^\star}} + \overrightarrow{x_{A_2^\star} x_{A_0^\star}}\Big) = \frac{1}{4}\overrightarrow{x_A x_\sigma} \wedge 0 = 0.$$

This ends the proof. □

We are now in a position to deduce the weak (dual) consistency claim for the 3D sd-NDD scheme, under the following mesh regularity assumption:

$$\begin{aligned}&\text{the angles } \theta^{\mathcal{D}_{A,\sigma,e}} \text{ between the dual faces } A_e^\star|B_e^\star \text{ and the vectors } \overrightarrow{x_{A_e^\star} x_{B_e^\star}}\\ &\text{are separated from zero, uniformly with respect to } A\in\mathfrak{M},\ \sigma\in\Sigma_A,\ e\in\mathcal{E}_\sigma,\\ &\text{uniformly for all meshes } \mathcal{T} \text{ in the considered family of meshes.}\end{aligned} \tag{5.20}$$

Proposition 5.3. *Denote by $\mathbb{P}^{\overline{\mathcal{T}}}$ the operator of projection of a smooth function on $\mathbb{R}^{\overline{\mathcal{T}}}$: for $\varphi\in C_0^\infty(\Omega)$, $\mathbb{P}^{\overline{\mathcal{T}}}\varphi$ has the entries $\varphi(x_K)$ at cells $K\in\mathfrak{M}\cup\mathfrak{M}^\star$, and zero values at boundary cells. Further, denote by $\mathbb{P}^{\mathfrak{D}}$ the following operator of projection of a smooth vector-field on $(\mathbb{R}^3)^{\mathfrak{D}^{sd}}$: for $\psi\in C^\infty(\Omega;\mathbb{R}^3)$, $\mathbb{P}^{\mathfrak{D}}\psi$ is assigned the entries*

$$\psi_{\mathcal{D}_{A,\sigma,e}} := \frac{1}{|\sigma|}\int_\sigma \psi, \quad \forall \mathcal{D}_{A,\sigma,e}\in\mathfrak{D}. \tag{5.21}$$

The 3D sd-NDD discrete divergence operator $\mathrm{div}^{\mathcal{T}}$ is consistent in the weak-$\star$ $W^{-1,\infty}$ sense, that is, for all sequence of meshes satisfying the regularity assumption (5.20), for all sequence $(\varphi^{\overline{\mathcal{T}}})_{\mathcal{T}}$, $\varphi^{\overline{\mathcal{T}}}\in\mathbb{R}_0^{\overline{\mathcal{T}}}$ with $\|\nabla^{\mathfrak{D}}\varphi^{\overline{\mathcal{T}}}\|_{L^1(\Omega)}\le const$, (2.13) holds true as the size $h^{\mathcal{T}}$ of $\mathcal{T}$ goes to zero

Proof. We follow the itinerary of the proof of Proposition 2.3, using Lemma 5.1 to transform the entries $\mathbb{P}^{\mathcal{T}}\big(\mathrm{div}\,\psi\big)|_{A^\star}$ into $\mathrm{div}_{A^\star}(\mathbb{P}^{\mathfrak{D}}\psi)$ plus an error term featuring the differences $\psi_{A,\sigma,e}^\star - \psi_\sigma$. In addition to the vector values given by (5.21) that we merely denote by ψ_σ because they do not depend on A, e, we introduce

$$\psi_{\mathcal{D}_{A,\sigma,e}} := \frac{1}{|\sigma_{A,\sigma,e}^\star|}\int_{\sigma_{A,\sigma,e}^\star} \psi, \quad \forall \mathcal{D}_{A,\sigma,e}\in\mathfrak{D};$$

we recall that $\sigma_{A,\sigma,e}^\star$ is the portion of the dual interface contained within $\mathcal{D}_{A,\sigma,e}$. We have, using the Green-Gauss theorem,

$$\begin{aligned}\mathbb{P}^{\mathcal{T}}\big(\mathrm{div}\,\psi\big)|_{A^\star} &= \frac{1}{|A^\star|}\sum_{A\in\mathfrak{M}_{A^\star}}\sum_{\sigma\in\Sigma_A}\sum_{e\in\mathcal{E}_\sigma^{A^\star}} \psi_{A,\sigma,e}^\star\cdot\mathbf{N}_{A,\sigma,e}^{A^\star}\\ &= \frac{1}{|A^\star|}\sum_{A\in\mathfrak{M}_{A^\star}}\sum_{\sigma\in\Sigma_A}\sum_{e\in\mathcal{E}_\sigma^{A^\star}} (\psi_{A,\sigma,e}^\star-\psi_\sigma)\cdot\mathbf{N}_{A,\sigma,e}^{A^\star} + \frac{1}{|A^\star|}\sum_{A\in\mathfrak{M}_{A^\star}}\sum_{\sigma\in\Sigma_A}\sum_{e\in\mathcal{E}_\sigma^{A^\star}} \psi_\sigma\cdot\mathbf{N}_{A,\sigma,e}^{A^\star}.\end{aligned}$$

Denote T_0, T_1 the two terms in the right-hand side of the above relation. Exploiting the fact that $\psi_{\mathcal{D}_{A,\sigma,e}} = \psi_\sigma$ does not depend on A, e, using Lemma 5.1 we are in a position to claim that the term T_1 coincides with $\mathrm{div}_{A^\star}\big(\mathbb{P}^{\mathfrak{D}}\psi\big)$. Indeed, first, there holds

$$T_2 := \frac{1}{|A^\star|}\sum_{A\in\mathfrak{M}_{A^\star}}\sum_{\sigma\in\Sigma_A}\sum_{e\in\mathcal{E}_\sigma} \psi_\sigma\cdot\mathbf{N}_{A,\sigma,e} = 0,$$

due to the cancellation of the terms $\psi_\sigma\cdot\mathbf{N}_{A,\sigma}$, $\psi_\sigma\cdot\mathbf{N}_{B,\sigma}$ coming from A, B such that $\sigma = A|B$. Second, owing to (5.16) and the fact that ψ_σ is independent of e, there holds

$$T_3 := \frac{1}{|A^\star|}\sum_{A\in\mathfrak{M}_{A^\star}}\sum_{\sigma\in\Sigma_A}\sum_{e\in\mathcal{E}_\sigma} \psi_\sigma\cdot\mathbf{N}_{A,\sigma,e}^{\#} = 0$$

Third, thanks to (5.17), ψ_σ being independent of e, in the term T_1 the inner sum $\sum_{e\in\mathcal{E}_\sigma^{A^\star}}\psi_\sigma\cdot\mathbf{N}_{A,\sigma,e}^{A^\star}$ can be substituted by $\sum_{e\in\mathcal{E}_\sigma^{A^\star}}\psi_\sigma\cdot\widetilde{\mathbf{N}_{A,\sigma,e}^{A^\star}}$. Finally, by virtue of the definition (5.14) of $\widehat{\mathbf{N}_{A,\sigma,e}^{\#}}$,

$$T_1=T_4+\frac{1}{2\#\nu_\sigma}(-T_2+T_3)\equiv\frac{1}{|A^\star|}\sum_{A\in\mathfrak{M}_{A^\star}}\sum_{\sigma\in\Sigma_A^{A^\star}}\Big\{\sum_{e\in\mathcal{E}_\sigma^{A^\star}}\psi_\sigma\cdot\widetilde{\mathbf{N}_{A,\sigma,e}^{A^\star}}+\sum_{e\in\mathcal{E}_\sigma}\psi_\sigma\cdot\widehat{\mathbf{N}_{A,\sigma,e}^{\#}}\Big\},$$

which coincides with the definition of $\operatorname{div}_{A^\star}\big(\mathbb{P}^{\mathfrak{D}}\psi\big)$ having in mind that $\psi_\sigma=\psi_{\mathcal{D}_{A,\sigma,e}}$ for all $A\in\mathfrak{M}$, $\sigma\in\Sigma_A$ such that $e\in\mathcal{E}_\sigma$.

Upon cancellations involving in particular the above term T_1, solely the terms originating from the expression of T_0 persist in the right-hand side of (2.13):

$$\begin{aligned}\Big[\!\Big[\operatorname{div}^{\mathcal{T}}\big(\mathbb{P}^{\mathfrak{D}}\psi\big)-\mathbb{P}^{\mathcal{T}}\big(\operatorname{div}\psi\big),\phi^{\mathcal{T}}\Big]\!\Big]&=\frac{1}{3}\sum_{A^\star\in\mathfrak{M}^\star}\sum_{A\in\mathfrak{M}_{A^\star}}\sum_{\sigma\in\Sigma_A}\sum_{e\in\mathcal{E}_\sigma^{A^\star}}(\psi_{A,\sigma,e}^\star-\psi_\sigma)\cdot\mathbf{N}_{A,\sigma,e}^{A^\star}\\&=\frac{1}{3}\sum_{A\in\mathfrak{M}}\sum_{\sigma\in\Sigma_A}\sum_{e\in\mathcal{E}_\sigma}(\varphi_{A_\sigma^\star}-\varphi_{B_\sigma^\star})(\psi_{A,\sigma,e}^\star-\psi_\sigma)\cdot\mathbf{N}_{A,\sigma}^\star;\end{aligned}$$

here, as usual, we have gathered the summation by diamonds using the conservativity of the dual fluxes given, in a diamond $\mathcal{D}_{A,\sigma,e}$, by $(\psi_{A,\sigma,e}^\star-\psi_\sigma)$. Now, $\psi_{A,\sigma,e}^\star-\psi_\sigma$ is order one small with respect to the size $h^{\mathcal{T}}$ of the mesh, because ψ is smooth. Dividing and multiplying by $|e|$, having in mind that $\left|\frac{\varphi_{B_e^\star}-\varphi_{A_e^\star}}{|e|}\right|\le const\,|\nabla_{\mathcal{D}_{A,\sigma,e}}\varphi^{\overline{\mathcal{T}}}|$ with the constant that only depends on the lower bound on the angle $\theta^{\mathcal{D}_{A,\sigma,e}}$ in (5.20), we deduce the required claim. □

The conclusions for the 3D sd-NDD scheme are the same as those for the fd-NDD version, outlined at the end of Section 5.2; the main difference between the schemes resides in the unconditional coercivity (validity of the discrete Poincaré inequality, irrespective of the values $\#\nu_\sigma$) for the sd-NDD method.

Remark 5.3. *Finally, note that if $\#\nu_\sigma=3$ for all faces of the mesh (e.g., for a simplicial mesh) the 3D fd- and sd-NDD schemes for* (1.1) *coincide provided the diffusion tensor in $x\mapsto\boldsymbol{\alpha}(x,\zeta)$ is discretized per fd-diamond $\mathcal{D}_{A,\sigma}$ (and not per smaller sd-diamond $\mathcal{D}_{A,\sigma,e}$).*

Indeed, whenever $\#\nu_\sigma=3$, both gradient reconstructions boil down to the unique $\mathbb{P}_1$ reconstruction over $\mathcal{D}_{A,\sigma}=\bigcup_{e\in\mathcal{E}_\sigma}\mathcal{D}_{A,\sigma,e}$. Moreover, the discrete divergence operators coincide on discrete fields constant per fd-diamond $\mathcal{D}_{A,\sigma}$. The latter fact can be obtained either from the relations (5.9), (5.16),(5.17)*, or by exploiting the discrete duality relation with arbitrarily chosen discrete test functions.*

6 Numerical experiments

In this section we provide numerical results for the 2D NDD scheme. The efficiency and the robustness of the method with respect to various meshes, physical inputs, nonlinearities, and discontinuities of the diffusion tensor are investigated by assessing the rate of convergence. A particular emphasis is placed on the scheme performance in the case of the p-Laplacian problem.

The model (1.1) is numerically solved using six different families of refined meshes on the computational domain that is fixed to the unit square $\overline{\Omega}=[0,1]^2$. They include typical difficulties such as nonconformity, distortion etc. They are mostly taken from the celebrated 2008 FVCA benchmark on anisotropic diffusion problems, see [26]. Following Fig. 3, we respectively label them with **Tri**, **RandQ**, **Kersh**, **LocRef**, **Cart** and **DistQ**.

The equations of the NDD numerical scheme (3.6) give rise to a nonlinear algebraic system that is solved thanks to Newton-Raphson's method. Given a sequence $(\boldsymbol{X}^n)_n$, let us denote $\boldsymbol{\delta}X^n=\boldsymbol{X}^{n+1}-\boldsymbol{X}^n$, for all $n\ge0$. The core of the Newton's algorithm is the resolution of the linear system of the form

$$\boldsymbol{A}(u_n^{\mathcal{T}})\boldsymbol{\delta}u\mathcal{T}_n=-\boldsymbol{F}(u_n^{\mathcal{T}}),\tag{6.1}$$

where $\boldsymbol{A}(u_n^{\mathcal{T}})$ accounts for the Jacobian matrix and $\boldsymbol{F}(u_n^{\mathcal{T}})$ stands for the residual function resulting from the numerical scheme (3.6). Before the resolution, the linear system (6.1) can be simplified, eliminating

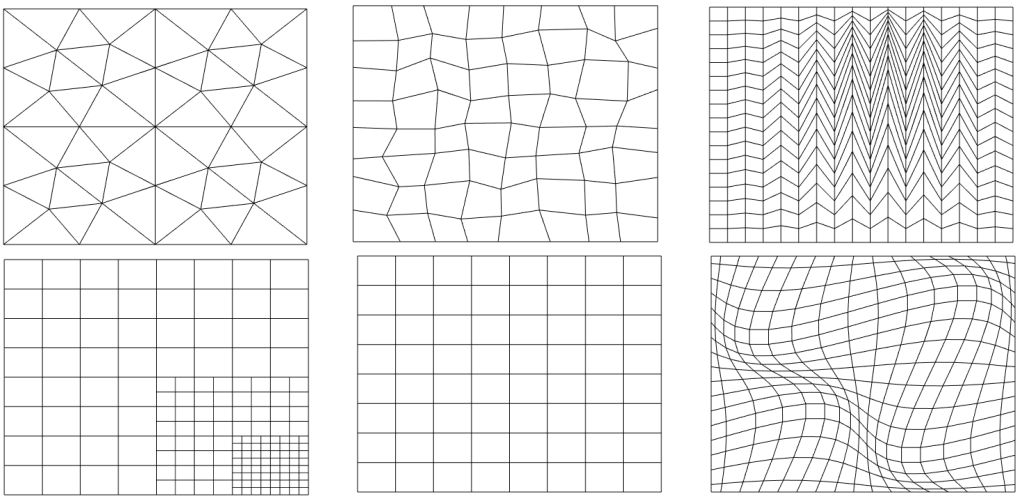

Figure 3: Meshes used in the numerical tests. From left to right: triangular, random quadrangular, Kershaw, locally refined, Cartesian and distorted quadrangular meshes.

the cell unknowns by the procedure highlighted in Section 3.4. Due to this modification of the scheme, the computational cost of the NDD method is greatly reduced in comparison to the DDFV methods, while keeping the advantage of an accurate gradient discretization. Accordingly, the solution to (3.6) is obtained as the limit to a sequence of iterates denoted by $(u_n^{\mathcal{T}})_{n\in\mathbb{N}}$. The convergence criterion is made on the successive iterates in the ℓ^2-norm as follows

$$\left\|u_{n+1}^{\mathcal{T}} - u_n^{\mathcal{T}}\right\|_{\ell^2} \leq 10^{-10}.$$

Let u_e denote the exact solution to (1.1), whenever it is given by an explicit formula. In most of the tests below, the performance of the proposed nodal scheme is quantified by measuring the following relative errors in the sense of L^p and (discrete) $W^{1,p}$ norms

$$\frac{||u_e - u_h||_{L^p(\Omega)}}{||u_e||_{L^p(\Omega)}}, \quad \frac{||u_e - u_h||_{W^{1,p}(\Omega)}}{||u_e||_{W^{1,p}(\Omega)}}. \tag{6.2}$$

6.1 Test case 1

In this first experiment, we consider a linear and homogeneous, anisotropic operator $\boldsymbol{\alpha}$. It is given by $\boldsymbol{\alpha}(x, \nabla u) = \Lambda \nabla u$, where Λ is the anisotropic diagonal tenor $\Lambda = \text{diag}(0.1,10)$ such that the ratio of anisotropy is 100. With these data, we manufacture the analytical solution to (1.1) as

$$u_e(x_1, x_2) = 16x_1(1 - x_1)x_2(1 - x_2), \quad \forall (x_1, x_2) \in \Omega.$$

The right hand side is then derived from this explicit solution, by substitution into (1.1). The exact solution is compared to numerical one produced by the NDD scheme (3.6) by evaluating the quantities (6.2) for each sequence of the considered meshes. The results are displayed on Fig. 4 in the log-log scale. As expected, a quadratic (resp. linear) convergence rate is obtained for the L^2- norm (resp. H^1-norm).

6.2 Test case 2

Next, we look at the behavior of the nodal scheme for the heterogeneous problem taking $\boldsymbol{\alpha}(x, \nabla u) = \Lambda(x)\nabla u$ where Λ is the heterogeneous (space-dependent) tensor

$$\Lambda = \begin{pmatrix} 2x_1^2 + x_2^2 & -x_1x_2 \\ -x_1x_2 & x_1^2 + 2x_2^2 \end{pmatrix}.$$

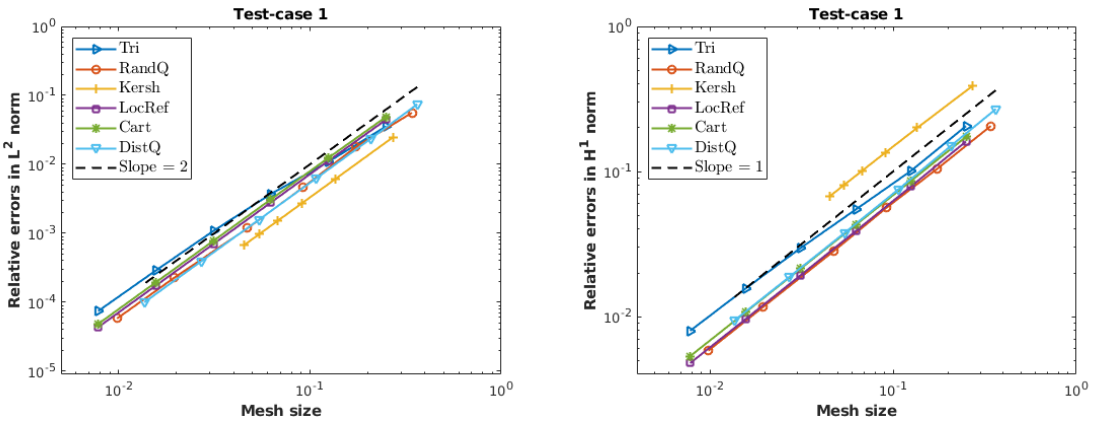

Figure 4: Test case 1: relative errors versus mesh size. Results are computed in the discrete L^2-norm (left) and H^1-norm.

We remind that the approximation of Λ is constant per diamond of the NDD scheme (one can also use a constant per primal cell approximation, being understood that each NDD diamond is included into a primal cell). The computations are carried out using the function

$$u_e(x_1, x_2) = \sin(\pi x_1)\sin(\pi x_2), \quad \forall (x_1, x_2) \in \Omega,$$

as an exact solution. Substituting Λ and u_e in the PDE in (1.1) yields the expression of f, which is a continuous function discretized by taking the cell and vertex values. The computed results are shown on Fig. 5. Similarly to the preceding test case, the accuracy is of second order for the solution and of first order for the gradient. A small reduction on the convergence rate is recorded on the first elements of the Kershaw meshes which may be induced by the distortion of the mesh and the heterogeneity of Λ.

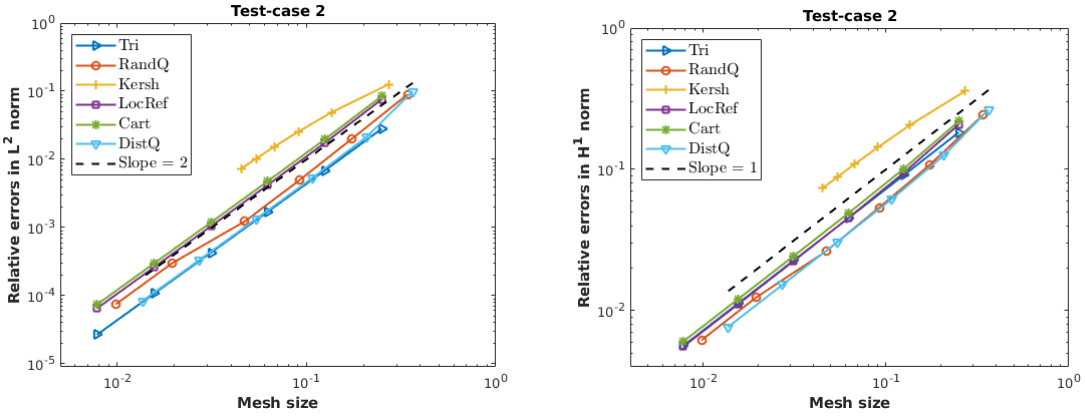

Figure 5: Test case 2: relative errors versus mesh size. Results are computed in the discrete L^2-norm (left) and H^1-norm.

6.3 Test case 3

We now inspect the behavior of our scheme in the homogeneous, isotropic but nonlinear situation with the p-Laplacian problem. Then, the expression of $\boldsymbol{\alpha}$ writes

$$\boldsymbol{\alpha}(x, \nabla u) = |\nabla u|^{p-2}\nabla u, \quad p \in (1, +\infty).$$

Setting $f = 2$, a two-dimensional solution to the p-Laplacian equation - with a non-homogeneous boundary condition, in a setting that goes beyond the basic setting of Sections 3,4 - is manufactured as follows

$$u_e(x) = p^\star \left(\frac{1}{(\sqrt{2})^{p^\star}} - |x - \widehat{x}|^{p^\star} \right), \quad \forall x = (x_1, x_2) \in \Omega,$$

where $\widehat{x} = (1/2, 1/2)$ and $p^\star = (p-1)/p$. The Dirichlet boundary condition agrees with the trace of u_e on $\partial\Omega$, it is taken into account in the gradient reconstruction in the same way as in the DDFV context of [8]. Observe that u_e lacks regularity around $\widehat{x}$. We run the nonlinear algorithm for three values of p. The results are exhibited on Figs. 6, 7, and 8 for $p = 1.5$, $p = 2$ and $p = 4$ respectively. In the case where $p \leq 2$, optimal convergence rates are achieved independently of the chosen mesh, i.e., we observe the order 2 for the solution and the order 1 for the gradient in the L^p-norm. Even if it is nonlinear, the term $|\nabla u|^{p-2}$ does not impact the accuracy of the scheme, see Fig. 6. This is no longer the case for $p > 2$, where a reduction on the orders of convergence is noticed (cf. Remark 4.2(i) and [8], see also [7]). Fig. 8 highlights this finding for $p = 4$. Indeed, as indicated in [19], the nonlinear flux term tends to vanish in regions where $|\nabla u|$ approaches 0. Hence, $\boldsymbol{\alpha}$ may act like a degenerate elliptic operator. This fact might be responsible on the observed lower regularity of the solution for large values of p.

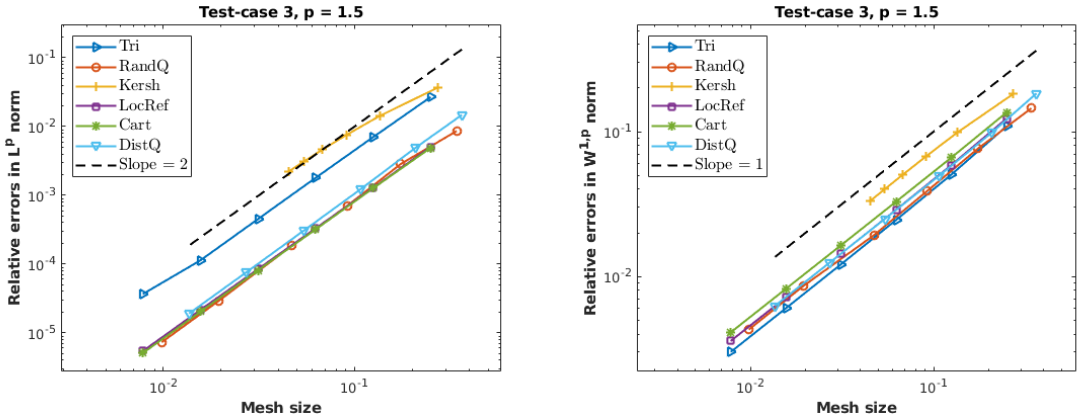

Figure 6: Test case 3: relative errors versus mesh size. Results are computed in the discrete L^p-norm (left) and $W^{1,p}$-norm with $p = 1.5$.

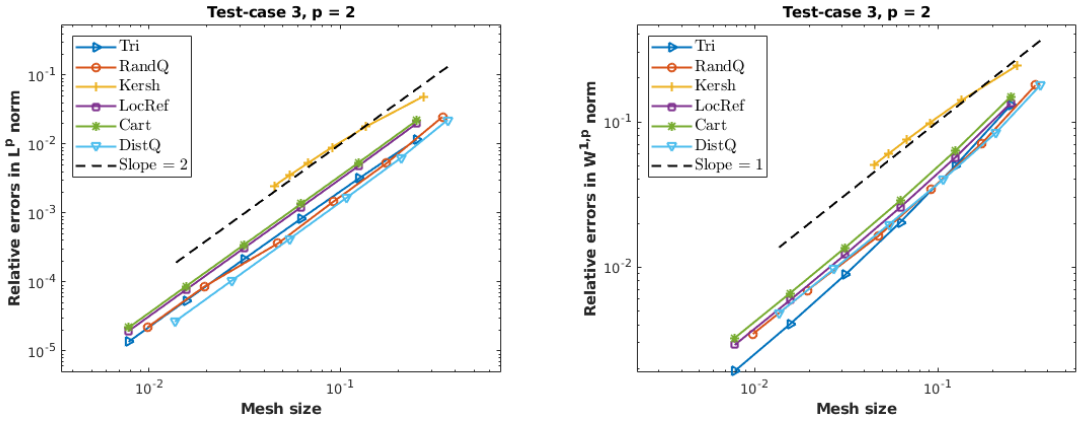

Figure 7: Test case 3: relative errors versus mesh size. Results are computed in the discrete L^p-norm (left) and $W^{1,p}$-norm with $p = 2$.

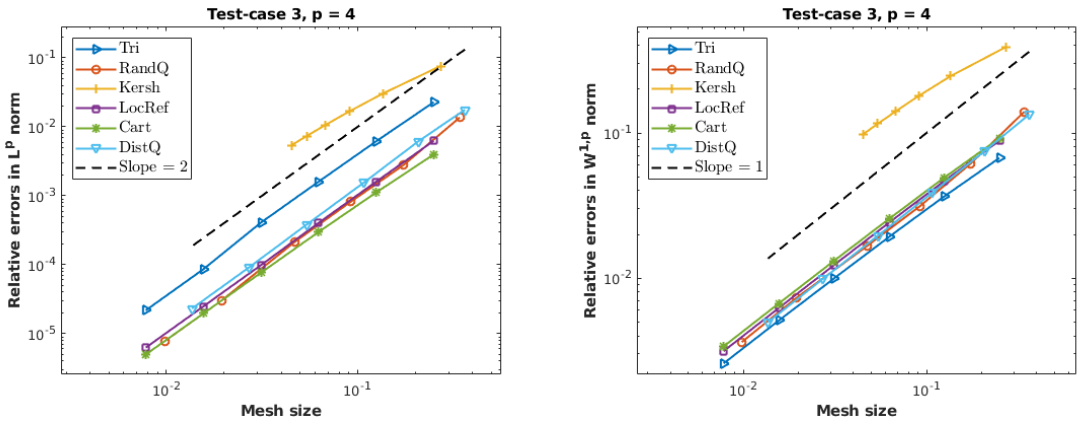

Figure 8: Test case 3: relative errors versus mesh size. Results are computed in the discrete L^p-norm (left) and $W^{1,p}$-norm with $p = 4$.

6.4 Test case 4

In this test, we keep the nonlinearity of p-Laplacian as in the previous example. We consider as the exact solution the function which gradient does not vanish on $\overline{\Omega}$:

$$u_e(x) = e^{x_1+\pi x_2}, \quad \forall x = (x_1, x_2) \in \Omega.$$

A nonhomogeneous Dirichlet boundary condition and a source term computed by substitution in the PDE in (1.1) correspond to this solution. We have run several tests with this set-up. Optimal convergence rates are maintained for $p \leq 2$. More importantly, for $p > 2$ the obtained convergence rates are enhanced with respect to those observed in Test 3. We plot on Fig. 9 the computed numerical convergence of the errors for $p = 5$. This improvement in the rates is linked to the regularity and the nondegeneracy of the solution. Note that it is known that problems for which the gradient does not vanish, or when it vanishes in a controlled way (cf. [10]), may even exibit superconvergence rates on symmetric meshes (cf. [7]).

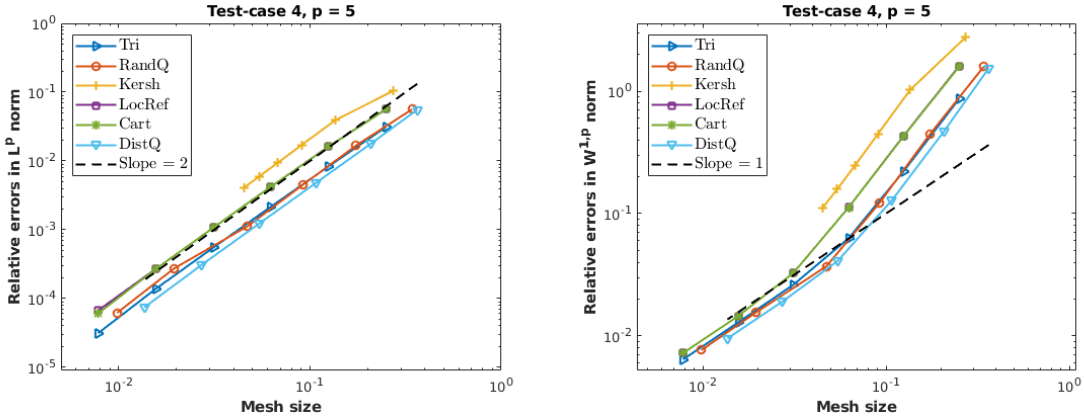

Figure 9: Test case 4: relative errors versus mesh size. Results are computed in the discrete L^p-norm (left) and $W^{1,p}$-norm with $p = 5$.

6.5 Test case 5

In this last test case, we are interested in the behavior of the nodal scheme in the presence of a strongly heterogeneous (discontinuous with respect to the space variable) anisotropic nonlinear flux function within

the p-Laplacian problem.

Let us define the following subsets

$$\Omega_1 = \{(x_1, x_2) \in \Omega / x_1 < 0.5\}, \quad \Omega_2 = \{(x_1, x_2) \in \Omega / x_1 > 0.5\},$$
$$\mathcal{U} = [0.1, 0.3] \times [0.1, 0.3] \bigcup [0.1, 0.3] \times [0.7, 0.9] \bigcup [0.7, 0.9] \times [0.1, 0.3] \bigcup [0.7, 0.9] \times [0.7, 0.9].$$

Being inspired by [11], the chosen operator $\boldsymbol{\alpha}$ takes the heterogeneous form

$$\boldsymbol{\alpha}(x, \nabla u) = \begin{cases} (\Lambda_1 \nabla u, \nabla u)^{\frac{p-2}{2}} \Lambda_1 \nabla u, & \text{if } x \in \Omega_1, \\ (\Lambda_2 \nabla u, \nabla u)^{\frac{p-2}{2}} \Lambda_2 \nabla u, & \text{if } x \in \Omega_2, \end{cases}$$

where Λ_1 and Λ_1 are the diagonal tensors

$$\Lambda_1 = \begin{pmatrix} 0.9 & 0 \\ 0 & 0.9 \end{pmatrix}, \quad \Lambda_2 = \begin{pmatrix} 0.5 & 0 \\ 0 & 0.3 \end{pmatrix}.$$

We consider the piecewise constant right hand side given by

$$f(x) = \begin{cases} 10 & \text{if } x \in \mathcal{U} \\ 0 & \text{if } x \in \Omega \setminus \mathcal{U} \end{cases}.$$

An illustration of f is depicted in Fig. 10. We impose the homogeneous Dirichlet boundary condition. The computed solution and its flux are supposed to be continuous across the interface $\partial\Omega_1 \cap \partial\Omega_2$ so that the straightforward NDD discretization with $\partial\Omega_1 \cap \partial\Omega_2$ included into a union of the primal mesh interfaces (cf. Remark 4.2(ii)) corresponds to the trivial Kirchhoff transmission conditions at the interface.

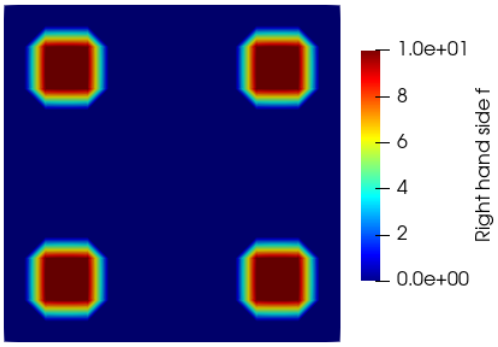

Figure 10: piecewise constant right hand side f used in the Test case 5.

In Fig. 11 we present the 2D view of surface plots of the solutions corresponding to three values of the exponent p, namely $p = 1.6, 3, 6$. The upper row shows the results of the simulation on the fifth Cartesian mesh. The lower one indicates the obtained results on the fifth locally refined mesh. We first observe that the both results are quite similar. The NDD scheme allows to excellently capture the whole complexity of phenomena expected in this test case. For instance, it is clearly seen that the numerical solution is more diffusive in Ω_1 than in Ω_2 as a result of the imposed anisotropy adjusted by the nonlinearity of the p-Laplacian operator. Moreover it is shown that the more p is increasing, the more the solution is lacking regularity.

7 Conclusion

In this work, we developed and analyzed a nodal discrete duality discretization in the context of nonlinear diffusion equations of Leray-Lions kind on general meshes. The scheme is designed to exploit the pros of the DDFV method and bypass its cons. Precisely, in contrast to the DDFV construction, the cell DOFs are

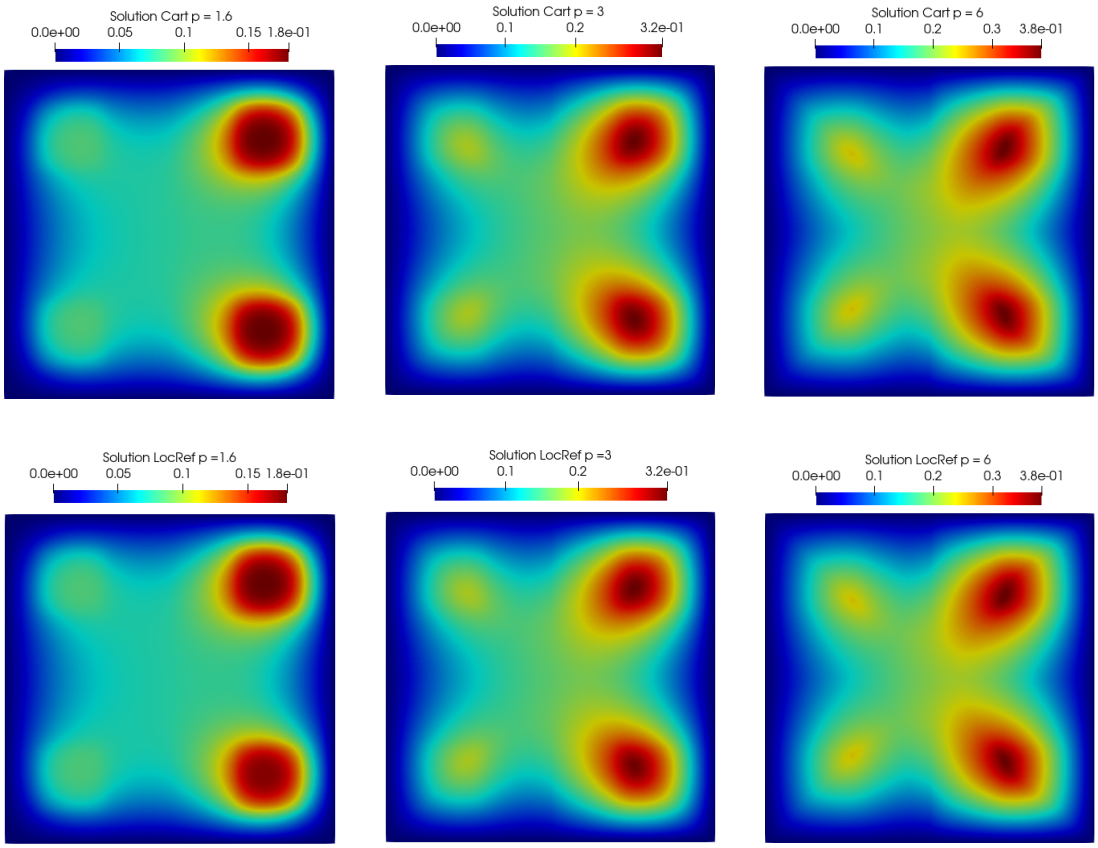

Figure 11: Test case 5 : computed results with a heterogeneous flux function on the fifth Cartesian mesh (top) and the fifth locally refined mesh (bottom) for $p = 1.6, p = 3, p = 6$.

eliminated without any fill-in, the spatial heterogeneity of the diffusion tensor is handled in straightforward way and there is no need to introduce some cumbersome penalization operators. On the other hand, even if the flux conservation is no longer fulfilled, due to the interpolation of the interface DOFs, the discrete duality property remains valid. The latter provides a key feature for the numerical analysis of the NDD scheme. As in the DDFV setting, two variants of the NDD methodology were proposed and discussed in 3D. A particular emphasis was placed on the consistency of the discrete gradient and divergence operator. The reported 2D numerical experiments disclose the expected accuracy and the robustness of the NDD scheme in different linear and nonlinear situations, covering the isotropic and anisotropic p-Laplacian test-cases.

Acknowledgment

This paper has been supported by the RUDN University Strategic Academic Leadership Program.

References

[1] M. Afif and B. Amaziane. Convergence of finite volume schemes for a degenerate convection-diffusion equation arising in flow in porous media. *Comput. Methods Appl. Mech. Engrg.*, 191(46):5265–5286, 2002.

[2] B. Andreianov, M. Bendahmane, and F. Hubert. On 3D DDFV discretization of gradient and divergence operators: discrete functional analysis tools and applications to degenerate parabolic problems. *Comput. Methods Appl. Math.*, 13(4):369–410, 2013.

[3] B. Andreianov, M. Bendahmane, F. Hubert, and S. Krell. On 3D DDFV discretization of gradient and divergence operators. I. Meshing, operators and discrete duality. *IMA J. Numer. Anal.*, 32(4):1574–1603, 2012.

[4] B. Andreianov, M. Bendahmane, and K. H. Karlsen. A gradient reconstruction formula for finite volume schemes and discrete duality. In *Finite volumes for complex applications V*, pages 161–168. ISTE, London, 2008.

[5] B. Andreianov, M. Bendahmane, and K. H. Karlsen. Discrete duality finite volume schemes for doubly nonlinear degenerate hyperbolic-parabolic equations. *J. Hyperbolic Differ. Equ.*, 7(1):1–67, 2010.

[6] B. Andreianov, F. Boyer, and F. Hubert. Besov regularity and new error estimates for finite volume approximations of the p-Laplacian. *Numer. Math.*, 100(4):565–592, 2005.

[7] B. Andreianov, F. Boyer, and F. Hubert. On the finite-volume approximation of regular solutions of the p-Laplacian. *IMA J. Numer. Anal.*, 26(3):472–502, 2006.

[8] B. Andreianov, F. Boyer, and F. Hubert. Discrete duality finite volume schemes for Leray-Lions-type elliptic problems on general 2D meshes. *Numerical Methods for Partial Differential Equations*, 23(1):145–195, 2007.

[9] B. Andreianov and E. H. Quenjel. Coercive and non-coercive discrete duality covolume schemes on general meshes. *In preparation.*

[10] J. W. Barrett and W. B. Liu. Finite element approximation of the p-Laplacian. *Math. Comp.*, 61(204):523–537, 1993.

[11] F. Boyer and F. Hubert. Finite volume method for 2D linear and nonlinear elliptic problems with discontinuities. *SIAM Journal on Numerical Analysis*, 46(6):3032–3070, 2008.

[12] K. Brenner and R. Masson. Convergence of a vertex centred discretization of two-phase Darcy flows on general meshes. *International Journal on Finite Volumes*, 10:1–37, 2013.

[13] K. Brenner, R. Masson, and E. H. Quenjel. Vertex Approximate Gradient Discretization preserving positivity for two-phase Darcy flows in heterogeneous porous media. *Journal of Computational Physics*, 409:109357, 2020.

[14] F. Brezzi, K. Lipnikov, and M. Shashkov. Convergence of the mimetic finite difference method for diffusion problems on polyhedral meshes. *SIAM J. Numer. Anal.*, 43(5):1872–1896, 2005.

[15] Z. Q. Cai. On the finite volume element method. *Numer. Math.*, 58(7):713–735, 1991.

[16] Y. Coudière and F. Hubert. A 3D discrete duality finite volume method for nonlinear elliptic equations. *SIAM J. Sci. Comput.*, 33(4):1739–1764, 2011.

[17] Y. Coudière, C. Pierre, O. Rousseau, and R. Turpault. A 2D/3D discrete duality finite volume scheme. Application to ECG simulation. *Int. J. Finite Vol.*, 6(1):24, 2009.

[18] K. Domelevo and P. Omnes. A finite volume method for the Laplace equation on almost arbitrary two-dimensional grids. *M2AN Math. Model. Numer. Anal.*, 39(6):1203–1249, 2005.

[19] J. Droniou. Finite volume schemes for fully non-linear elliptic equations in divergence form. *ESAIM: Mathematical Modelling and Numerical Analysis*, 40(6):1069–1100, 2006.

[20] J. Droniou. Finite volume schemes for diffusion equations: introduction to and review of modern methods. *Math. Models Methods Appl. Sci.*, 24(8):1575–1619, 2014.

[21] J. Droniou, R. Eymard, T. Gallouët, C. Guichard, and R. Herbin. *The gradient discretisation method*, volume 82 of *Mathématiques & Applications (Berlin) [Mathematics & Applications]*. Springer, Cham, 2018.

[22] J. Droniou, R. Eymard, and R. Herbin. Gradient schemes: generic tools for the numerical analysis of diffusion equations. *ESAIM Math. Model. Numer. Anal.*, 50(3):749–781, 2016.

[23] L. C. Evans. *Partial differential equations*, volume 19. American Mathematical Society, 2010.

[24] R. Eymard, C. Guichard, R. Herbin, and R. Masson. Vertex-centred discretization of multiphase compositional darcy flows on general meshes. *Computational Geosciences*, 16(4):987–1005, 2012.

[25] R. Eymard and R. Herbin. Gradient scheme approximations for diffusion problems. In *Finite volumes for complex applications VI. Problems & perspectives. Volume 1, 2*, volume 4 of *Springer Proc. Math.*, pages 439–447. Springer, Heidelberg, 2011.

[26] R. Herbin and F. Hubert. Benchmark on discretization schemes for anisotropic diffusion problems on general grids. In R. Eymard and J.-M. Herard, editors, *Finite Volumes for Complex Applications V*, pages 659–692. Wiley, 2008.

[27] F. Hermeline. Une méthode de volumes finis pour les équations elliptiques du second ordre. *C. R. Acad. Sci. Paris Sér. I Math.*, 326(12):1433–1436, 1998.

[28] F. Hermeline. A finite volume method for the approximation of diffusion operators on distorted meshes. *J. Comput. Phys.*, 160(2):481–499, 2000.

[29] F. Hermeline. A finite volume method for approximating 3D diffusion operators on general meshes. *J. Comput. Phys.*, 228(16):5763–5786, 2009.

[30] J. Leray and J.-L. Lions. Quelques résultats de Višik sur les problèmes elliptiques non linéaires par les méthodes de Minty-Browder. *Bulletin de la S. M. F.*, 93:97–107, 1965.

[31] J.-L. Lions. *Quelques méthodes de résolution des problèmes aux limites non linéaires*. Dunod, Paris; Gauthier-Villars, Paris, 1969.

[32] K. Lipnikov, G. Manzini, and M. Shashkov. Mimetic finite difference method. *J. Comput. Phys.*, 257(part B):1163–1227, 2014.

[33] G. J. Minty. On a „monotonicity" method for the solution of nonlinear equations in banach spaces. *Proceedings of the National Academy of Sciences of the United States of America*, 50(6):1038, 1963.

[34] E. H. Quenjel and A. Beljadid. Node-diamond approximation of heterogeneous and anisotropic diffusion systems on arbitrary two-dimensional grids. *Preprint*, 2021.